P.94

NASA CONTRACTOR REPORT

NASA CR-19

N63 21897

NASA CR-19

RESEARCH STUDY ON THE ACCELERATION HODOGRAPH AND ITS APPLICATION TO SPACE TRAJECTORY ANALYSIS

Prepared under Contract No. NASw-565 by
UNITED AIRCRAFT
Farmington, Connecticut

NATIONAL AERONAUTICS AND SPACE ADMINISTRATION • WASHINGTON, D. C. • SEPTEMBER 1963

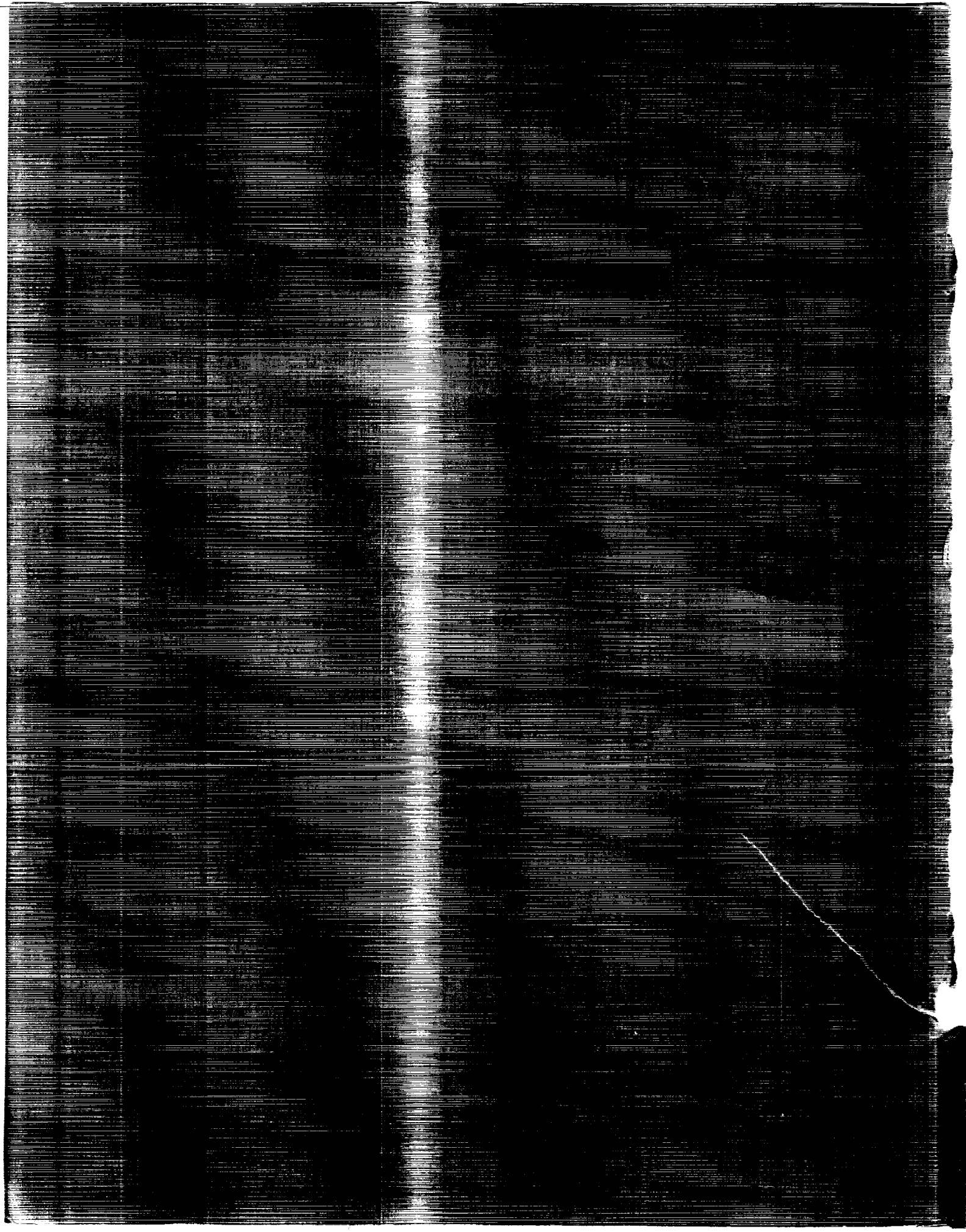

NASA CONTRACTOR REPORT CR-19

RESEARCH STUDY ON THE ACCELERATION HODOGRAPH AND ITS APPLICATION TO SPACE TRAJECTORY ANALYSIS

Prepared under Contract No. NASw-565 by
UNITED AIRCRAFT CORPORATION
Farmington, Connecticut

for

NATIONAL AERONAUTICS AND SPACE ADMINISTRATION

TABLE OF CONTENTS

TABLE OF CONTENTS (contd.)

ILLUSTRATIONS

LIST OF TABLES

FOREWORD

This final report presents the results of research conducted for NASA Headquarters under Contract No. NASw-565 dated December 1, 1962. This study contract was awarded in response to the United Aircraft Corporate Systems Center Proposal No. SCP 6211 dated May 4, 1962. The original proposed scope was revised to cover the research topics outlined in Section II of this report.

SUMMARY

In this study, the acceleration hodograph was used to obtain transformed equations of motion for a propelled space vehicle subject to the gravitational attraction of one major celestial body, in two-dimensional space. Basic definitive relations were determined, which are convenient for thrust program synthesis and trajectory analysis.

It is shown that the acceleration hodograph of an orbit (i.e., a ballistic trajectory) is a form of the limaçon. The acceleration limaçon and the hodograph equations of motion enable a direct graphical representation of the thrust program, as well as space, velocity, and acceleration coordinates of the trajectory. The hodograph equations describe the space vehicle motion with thrust, by a continuum of instantaneous orbital hodographs. Consequently, upon thrust termination for any reason and at any instant of time, the hodograph equations provide the subsequent ballistic trajectory directly. Machine solution of the hodograph equations requires only one integration of first-order, nonlinear differential equations, while the classical equations require two integrations of second-order, nonlinear differential equations.

The space trajectory obtainable with one class of thrust program has been analyzed by use of the hodograph equations of motion and associated relations. This thrust program, which is being studied for potential lunar landing applications, resulted in acceleration hodograph equations of trigonometric form. While the desired closed-form analytic solution was not obtained, the current study results indicate that such analytic solution may yet be achieved. United Aircraft machine solution of the hodograph equations provided excellent correlation with the NASA machine solution of the classical equations, except in the close neighborhood of the terminal point. The terminal point itself is singular in the hodograph transformation, since the terminal velocity is zero. In addition, the current study results have revealed previously unsuspected trajectory characteristics useful for future study, thrust program application, and system mechanization.

Future advanced study of the transformation technique has been recommended in the basic areas of extension of the application techniques, investigation of the basic characteristics of the application equations, computation and optimization techniques with hodograph equations, and further analysis of the specified lunar landing thrust program. In extension of the application techniques, formulation of the three-dimensional equations, analytical treatment of oblateness effects, and analytical treatment of drag or other resistive force effects are paramount. Investigation of the basic characteristics of the application equations should result in hodograph generation techniques, so that analytic integration would be unnecessary. System mechanization techniques such as situation displays and abort emergency command and control may also be greatly facilitated by the use of the hodograph equations of motion.

I. STUDY BACKGROUND

The synthesis and analysis of trajectories for powered space vehicles is a relatively new and only partially understood branch of space technology. While the general equations of motion can be defined rigorously for subsequent computation by high-speed and large-scale digital computers, such equations and the associated computation processes are usually quite extensive, complex, and intractable for preliminary design study to determine system feasibility. That is, the required time and cost of such generalized treatment of the space trajectory problem area are usually prohibitive for effective system analysis of new concepts pertaining to new mission requirements. Equally important, such mechanical treatment provides little understanding of the underlying criteria and performance characteristics as a function of the physical principles. In view of the currently very incomplete analytic knowledge of space trajectory classes of solution, this deficiency may become increasingly serious and restrictive in the development of advanced and more versatile space vehicle subsystems and detailed planning of space mission operations.

In recent years, analytic knowledge of the classes of ballistic trajectory solutions (or the families of trajectories) has been effectively applied to trajectory analysis by use of the variation-of-parameters method. With this technique, a nominal trajectory (or trajectory class) is defined by suitable orbital parameters. Then trajectories definable within this trajectory class may be studied by considering their variations from the nominal trajectory. These variations may be due to observational errors, perturbation forces, or thrust forces. In classical celestial mechanics, the conic parameters, which define planar, unperturbed orbital figures, have been used most widely. However, the resultant equations for given space system applications are complex, and singularities are encountered within regions of practical interest. Consequently, transformations of variables (or parameters) have been proposed, which "regularize" the equations and provide equation forms which are more tractable for analysis of space trajectories, e.g., Herrick's "universal" parameters.

Heretofore, the variation-of-parameters analysis technique has been effective principally for ballistic motion in the two-body problem formulation, since the nature of these orbital classes has been completely analyzed and understood. However, the variation-of-parameters method has not yet been effectively extended to the N-body problems since little is known about the properties of such trajectory classes.

Upon application of an onboard thrust vector, variable in magnitude or direction, the analysis[1] and synthesis[2] of vehicle motion (within the gravitational field of one major celestial body) are most usually based upon extensions of the celestial mechanics techniques proven for ballistic trajectories. Many such analyses and syntheses are based upon the variation-of-parameters method. However, most presently available techniques are usually deficient in significant respects, and the results are often approximations at best. These techniques are especially deficient in providing effective synthesis of a thrust program to obtain a desired space trajectory. That is, which thrust programs (or thrust controller functions) and parametric values thereof will provide the desired trajectory? Moreover, for a finite number of feasible but different programs (and hence, different sets of parametric values), what are the relative values of each program, and/or the significant tradeoffs which characterize them? Also, what controller function characteristics are most significant or critical?

Such considerations led to the study of the velocity hodograph transformation and subsequent development of its synthesis (Ref. 1-10). Initially, the research phase consisted of investigation of the transformation properties, resulting in complete analytic definition of basic equations and transformation mapping relations. Subsequently, the development phase consisted of the application of optimization conditions and trajectory constraints to identify the permissible trajectory classes. Unlike many other current space trajectory study programs, one of the more important aspects of the hodograph approach is that machine computation is not a basic element of the investigation. Consequently, analytic rigor can be effectively attained or explicitly examined.

The existence of the velocity hodograph transformation and its utility in synthesis of impulsive thrust programs led to speculation (Ref. 1, 11, 12) on the existence of an acceleration hodograph transformation which might prove useful for the synthesis of continuous, as well as impulsive, thrust programs. Such a transformation would enable the consideration of acceleration sensor subsystems for orbit determination and/or control. In addition, it would provide an analytic basis for comparison of impulsive vs continuous thrust programs where these would otherwise meet all dynamics constraints for space trajectories. In general, only the basic definitive equations and synthesis process sufficient to enable the application to study of one specified thrust program have been developed.

---

[1] Analysis of the generated path, for a vehicle subject to specified constraints, will provide definitive equations of motion and predict associated data not observed directly.

[2] Synthesis of the thrust program (i.e., thrust vector as a function of time), for a vehicle subject to specified constraints, will provide a desired generated path from the synthesized equations of motion.

II. SCOPE OF STUDY

The basic objectives of the research study under Contract NASw-565 were the investigation and definition of the acceleration hodograph and its application to the synthesis of space trajectories, with the latter objective limited to the study of one thrust program class. The gravitational potential field function was assumed to be due to a regular, spherical celestial body. Consequently, in this initial study the research effort was limited to two-dimensional (or planar) motion. However, if the study results for the two-dimensional problem were to be found promising, extension to three-dimensional space and/or potential fields with harmonic content could be considered in a subsequent research effort.

A thrust program specified by the Langley Research Center was to be expressed in terms of the acceleration hodograph parameters, to obtain an analytic trajectory solution in closed form. In the given problem, the thrust vector was always constrained to be directed opposite to the instantaneous velocity vector, so as to generate a descent trajectory from lunar orbit to zero velocity at a relatively low altitude above the lunar surface. This thrust program application is described in detail in Appendix A.

The thrust program may be specified as a function of time, or of one or more state variables. For example, a navigation subsystem, which operates explicitly to provide an open-loop input to the control subsystem, will require a thrust program defined as a function of time. However, a closed-loop navigational mode of operation will use a thrust program defined as a function of a state variable such as positional or velocity error along the path. Although the open-loop mode is the most primitive class of operation, the research study has been restricted to consideration of thrust programs explicitly dependent upon time. Obviously, effective synthesis and analysis of such programs can subsequently be reconsidered for closed-loop operation, if the time-dependent solutions are known.

The hodograph transformation has been found extremely effective in past applications because the transformed equations of motion are comprised of simple functions of the spherical trigonometry. Consequently, all state constraints can be defined without time in explicit form. Then, for example, the constraints of position and velocity coordinates upon orbital transfer can be presented graphically by planar geometric relations. However, the formulation of state variables as a function of time, in the transformed equations of motion, has not yet been explored comprehensively. As a result, the research study reported herein has been principally concerned with solutions obtained upon integration of the acceleration hodograph equations, rather than the explicit generation of the acceleration hodograph of the powered trajectory. That is, the integration of the acceleration hodograph equations would provide the solution as a function of the instantaneous velocity hodograph, which defines the space and velocity coordinates completely.

It should be noted that use of the hodograph equations requires integration of first order, nonlinear differential equations only, rather than of the second order, nonlinear differential equations of classical celestial mechanics. This fact, of course, appreciably reduces the complexity of the computer programming and the required computation time. Explicit generation of the acceleration hodograph would also define those coordinates completely, by virtue of the instantaneous acceleration hodograph and its mapping relations.

III. BACKGROUND SUMMARY OF DYNAMICS PRINCIPLES

Prior to derivation of the orbital equations of motion in terms of convenient space and velocity coordinates (see next Section), the following summary of the basic dynamics principles substantiates the analytic derivation of the orbital trajectory in the presence of applied forces, rather than for the simple ballistic case alone. This reference material is attributed to Reference 13, pp. 18-21.

A. D'Alembert's Principle

D'Alembert's principle results in Lagrange's equations

$$\frac{d}{dt}\left(\frac{\partial U}{\partial \dot{q}_i}\right) - \frac{\partial U}{\partial q_i} = Q_i \tag{1}$$

where

U = system kinetic energy of orbital point mass motion
Q_i = generalized force component in the q_i-coordinate.

B. Lagrange's Equations for a Conservative System

When $Q_i = -\dfrac{\partial V}{\partial q_i}$,

as for a conservative system when the forces are derivable from a scalar potential function V, then Lagrange's equations become

$$\frac{d}{dt}\left(\frac{\partial L}{\partial \dot{q}_i}\right) - \frac{\partial L}{\partial q_i} = 0 \tag{2}$$

where

$L=U-V$ = the "Lagrangian" of the system.

C. Lagrange's Equations for a Velocity-Dependent Potential

The previous paragraph described the system motion when the potential is a function of the position coordinate only. When the generalized forces are obtainable from a function $W(q_i, \dot{q}_i)$, then the same basic form of equation is preserved, as expressed by

$$\frac{d}{dt}\left(\frac{\partial W}{\partial \dot{q}_i}\right) - \frac{\partial W}{\partial q_i} = Q_i \tag{3}$$

where

$$L = U - W.$$

That is, W≡V. The term W is also described as a velocity dependent potential.

D. Lagrange's Equations for a Dissipation Function

It is interesting, although not directly pertinent in this research study, to note that

$$\frac{d}{dt}\left(\frac{\partial L}{\partial \dot{q}_i}\right) - \frac{\partial L}{\partial q_i} = Q_i \tag{4}$$

where

L contains the conservative potential function,

and

Q_i represents the nonpotential forces, such as frictional.

In this instance, Q_i is described as a dissipation function, where the forces may be frictional in nature. This would be the case for atmospheric drag, for example, or passage through an interplanetary gas cloud.

In the present study, Lagrange's equations for a conservative system will be obtained by use of the Lagrangian for the vehicle system. As an alternative, the principle of linear momentum (Newton's Second Law of Motion) may be used to obtain the orbital equations of motion; i.e., the time rate of change of the linear momentum of the vehicle rigid-body system is equal to the vector sum of the external forces.

In the present problem, the gravitational force of attraction due to the external source is derivable from the scalar potential field function of the celestial body. The thrust force is provided by the expansion of gases, accompanied by a change in the vehicle system mass. Since the entire mass-rate change of the vehicle system (as considered in this research study) is entirely related to the rocket thrust force, the mass change indicated by the Lagrangian or momentum treatments will not be present in the final equations of motion (Ref. 14).

IV. GENERAL EQUATIONS OF MOTION

A. Derivation with the Lagrangian

The Lagrangian of the complete space vehicle is

$$L = U - V = \frac{m}{2}\left[(\dot{r})^2 + (r\dot{\nu})^2\right] + \frac{\mu m}{r} \tag{5}$$

where r, ν, and m comprise the set of generalized coordinates q_i. The velocity components are functions of the radius scalar and the direction angle, as shown in Figure 1. Note that the Lagrangian (per unit-mass)

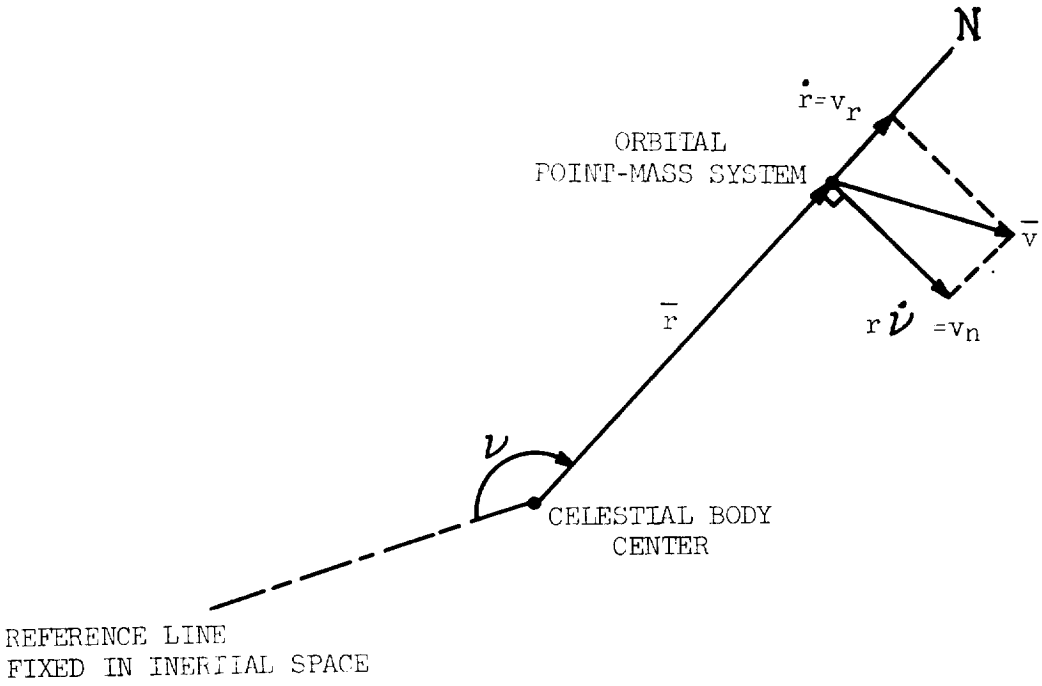

Fig. 1 Vector Definition of the Vehicle State in Inertial Space

$$\tilde{L} = \tilde{U} - \tilde{V} = \frac{1}{2}\left[(\dot{r})^2 + (r\dot{\nu})^2\right] + \frac{\mu}{r} \tag{6}$$

is independent of the mass change, so that mass would no longer comprise a generalized coordinate in this specific mass formulation.

For the r-coordinate: $\frac{\partial L}{\partial r} = mr\dot{\nu}^2 - \frac{\mu m}{r^2}$ (7)

$$\frac{\partial L}{\partial \dot{r}} = m\dot{r} \tag{8}$$

$$\frac{d}{dt}\left(\frac{\partial L}{\partial \dot{r}}\right) = m\ddot{r} + \dot{m}\dot{r} \tag{9}$$

$$\therefore \dot{m}\dot{r} + m\ddot{r} - mr\dot{\nu}^2 + \frac{\mu m}{r^2} = Q_r \tag{10A}$$

or

$$\left(\frac{\dot{m}}{m}\right)\dot{r} + \ddot{r} - r\dot{\nu}^2 + \frac{\mu}{r^2} = \frac{Q_r}{m} \tag{10B}$$

For the ν-coordinate:

$$\frac{\partial L}{\partial \nu} = 0 \tag{11}$$

$$\frac{\partial L}{\partial \dot{\nu}} = mr^2\dot{\nu} \tag{12}$$

$$\frac{d}{dt}\left(\frac{\partial L}{\partial \dot{\nu}}\right) = \dot{m}r^2\dot{\nu} + 2mr\dot{r}\dot{\nu} + mr^2\ddot{\nu} \tag{13}$$

$$\therefore \dot{m}r^2\dot{\nu} + 2mr\dot{r}\dot{\nu} + mr^2\ddot{\nu} = Q_\nu \tag{14A}$$

or

$$\left(\frac{\dot{m}}{m}\right)r\dot{\nu} + 2\dot{r}\dot{\nu} + r\ddot{\nu} = \frac{Q_\nu}{mr} \tag{14B}$$

For the m-coordinate:

$$\frac{\partial L}{\partial m} = \frac{1}{2}\left[(\dot{r})^2 + (r\dot{\nu})^2\right] + \frac{\mu}{r} \tag{15}$$

$$\frac{\partial L}{\partial \dot{m}} = 0 \tag{16}$$

so that

$$\frac{1}{2}\left[(\dot{r})^2 + (r\dot{\nu})^2\right] + \frac{\mu}{r} = Q_m \tag{17}$$

Consequently, although the vehicle system mass changes with time, no new information is provided. That is, Equation 17 shows that $Q_m \equiv \tilde{L}$, although the mass-rate change is constrained to the mass-flow law arbitrarily selectable. For example, in the lunar landing problem application here, the mass-flow rate is constant. Then

$$\dot{m} = k \tag{18}$$

$$\int_{m_0}^{m} dm = \int_{0}^{t} k \, dt \tag{19A}$$

$$m - m_0 = kt \tag{19B}$$

or

$$m = m_0 + kt, \tag{19C}$$

where k is negative in sign.

According to the momentum equation for rocket motion (Ref. 15),

$$m\Delta a = -\dot{m} v_g \equiv T \tag{20}$$

so that

$$m\Delta a_r = -\dot{m} v_{gr} \tag{21}$$

and

$$m\Delta a_\nu = -\dot{m} v_{g\nu} \tag{22}$$

But in general,

$$f = \dot{m}\dot{s} + m\ddot{s} \tag{23}$$

so that

$$f_r \equiv Q_r = \dot{m}\dot{r} - \dot{m} v_{gr} \tag{24}$$

$$f_\nu \equiv \frac{Q_\nu}{r} = \dot{m} r \dot{\nu} - \dot{m} v_{g\nu} \tag{25}$$

Consequently,

$$\ddot{r} - r\dot{\nu}^2 + \frac{\mu}{r^2} = -\left(\frac{\dot{m}}{m}\right) v_{gr} \equiv \frac{F_r}{m} \tag{10C}$$

$$2\dot{r}\dot{\nu} + r\ddot{\nu} = -\left(\frac{\dot{m}}{m}\right) v_{g\nu} \equiv \frac{F_\nu}{m} \tag{14C}$$

The resultant vector equation of motion is then seen to be

$$\Delta\bar{a} = \frac{\bar{F}}{m} = \left(\ddot{r} - r\dot{\nu}^2 + \frac{\mu}{r^2}\right)\bar{\imath} + \left(2\dot{r}\dot{\nu} + r\ddot{\nu}\right)\bar{\jmath} \tag{26}$$

B. Derivation with the Momentum Principle

According to the principle of linear momentum,

$$\bar{f} = \frac{d}{dt}(m\bar{v}) \tag{27}$$

Also, in vector form,

$$\dot{\bar{r}} = (\dot{r})\bar{\imath} + (r\dot{\nu})\bar{\jmath} \tag{28}$$

$$m\bar{v} = m\dot{\bar{r}} = (m\dot{r})\bar{\imath} + (mr\dot{\nu})\bar{\jmath} \tag{29}$$

$$\bar{f} = (\dot{m}\dot{r}\bar{\imath} + m\ddot{r}\bar{\imath} + m\dot{r}\dot{\nu}\bar{\jmath}) + \\ + (\dot{m}r\dot{\nu}\bar{\jmath} + m\dot{r}\dot{\nu}\bar{\jmath} + mr\ddot{\nu}\bar{\jmath} - mr\dot{\nu}^2\bar{\imath}) \tag{30A}$$

$$\bar{f} = (\dot{m}\dot{r} + m\ddot{r} - mr\dot{\nu}^2)\bar{\imath} + (\dot{m}r\dot{\nu} + 2m\dot{r}\dot{\nu} + mr\ddot{\nu})\bar{\jmath} \tag{30B}$$

$$\frac{\bar{f}}{m} = \left[\left(\frac{\dot{m}}{m}\right)\dot{r} + \ddot{r} - r\dot{\nu}^2\right]\bar{\imath} + \left[\left(\frac{\dot{m}}{m}\right)r\dot{\nu} + 2\dot{r}\dot{\nu} + r\ddot{\nu}\right]\bar{\jmath} \tag{31}$$

It is seen that Equation 30 is the vector form for Equations 10B and 14B. Consequently, the derivation results with the momentum principle are identical with those from the Lagrangian.

V. VELOCITY HODOGRAPH PARAMETERS OF AN ORBIT

Although the velocity hodograph parameters of an orbit have been previously derived and discussed at length (Ref. 1, 4, 5), the basic formulation of these hodograph parameters will be recapitulated in standardized symbology deemed more suitable for extension to the acceleration hodograph.

Let us consider the total energy equation for the vehicle rigid-body system in orbit, treated as a point-mass:

$$E = \frac{mv^2}{2} + V(r) \tag{32}$$

For the inverse-square potential field of gravitational attraction,

$$V(r) = -\frac{\mu m}{r} \tag{33}$$

so that

$$E = \frac{mv^2}{2} - \frac{\mu m}{r} \tag{34A}$$

is the instantaneous energy equation of the orbital system, such that E, m, v, r may be functions of time, but μ is always constant. If the system is conservative (or in ballistic flight), then E and m are constant. As before, let us resolve the velocity vector $\bar{v}$ (see Fig. 1) into the orthogonal components of a rotating polar coordinate system with origin at the vehicle center-of-mass, so that

$$E = \frac{m}{2}(v_r^2 + v_n^2) - \frac{\mu m}{r} \tag{34B}$$

or

$$E = \frac{m}{2}\left[(\dot{r})^2 + (r\dot{\nu})^2\right] - \frac{\mu m}{r} \tag{34C}$$

Since, in the conservative system,

$$\ell = m r v_n = \text{ constant} \tag{35}$$

let

$$C = \frac{\mu m}{\ell} = \frac{\mu}{r v_n} = \frac{\mu}{r^2 \dot{\nu}} \tag{36}$$

Then

$$\frac{2E}{m} = v_r^2 + v_n^2 - 2Cv_n \tag{34D}$$

or

$$\frac{2E}{m} + C^2 = v_r^2 + (v_n - C)^2 \tag{34E}$$

This equation defines a circle whose center is located at the distance C along the positive V_n-axis, with radius

$$R=\left(\frac{2E}{m}+C^2\right)^{\frac{1}{2}} \tag{37}$$

It is most convenient to refer the direction angle to the radius line through perigee passage (i.e., closest approach to the celestial body). Consequently, for an instantaneous orbit, and its hodograph,

$$v_r = \dot{r} = R\sin\phi \tag{38A}$$

$$v_n = r\dot{\nu} = C+R\cos\phi \tag{39A}$$

and

$$v = (C^2+R^2+2CR\cos\phi)^{\frac{1}{2}} \tag{40}$$

Note that v_r and v_n are defined in inertial space, although the true anomaly ϕ (referred to the perigee passage for the instaneous orbit) is used to describe their scalar magnitude (as shown by Equations 38A and 39A). Consequently, the energy equation can be presented in terms of the instantaneous parameters (C,R) and the true anomaly ϕ. If the system is conservative so that E and m are constant, then the angular momentum ℓ is constant, as noted previously. As a result, the parameters C,R are also constant terms which can be used to define the orbital velocity vector.

The locus of the velocity vector terminal point with the velocity vector initial point fixed in space describes a curve defined as the velocity hodograph of the orbit.[1] In the middle of the 19th century, Hamilton and Möbius showed that the velocity hodograph of the planar orbit is a circle in inertial space (Ref. 16, 17). Also, the velocity hodograph may be presented in complete three-dimensional vector notation (Ref. 18). Although the hodograph parameters have here been defined by use of a rotating polar coordinate system with its origin at the vehicle center-of-mass, the hodograph in inertial space is shown to be defined by these same parameters, upon reference to Figure 2. In a rectilinear coordinate system with origin located at the celestial body center-of-mass, and the apsidal line used as the direction angle reference,

$$v_X = v_n\sin\phi - v_r\cos\phi = C\sin\phi \tag{41}$$

$$v_Y = v_n\cos\phi + v_r\sin\phi = R + C\cos\phi \tag{42}$$

so that

$$v_X^2 + (v_Y - R)^2 = C^2 \tag{43}$$

[1] The unabridged definition (Webster's New International Dictionary, 2nd Edition Unabridged, G. & C. Merriam, 1958) of the hodograph of a variable vector is as follows: The locus of one end of a radius vector (the other end being fixed) that represents in magnitude and direction the rate of change of the variable vector.

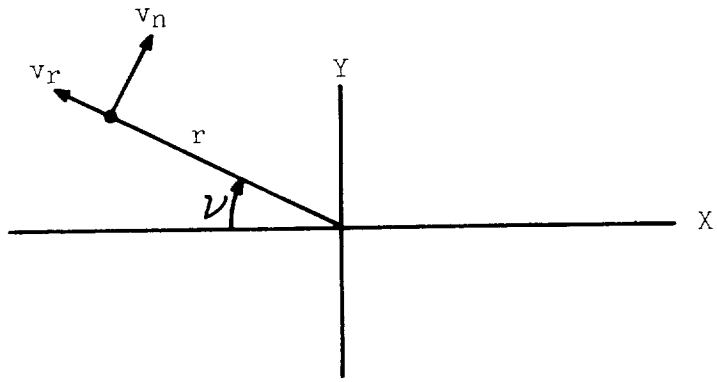

Fig. 2 Velocity Vector Definition in Inertially-Fixed Rectilinear Coordinates

Conversely, note that

$$v_r = v_Y \sin\phi - v_x \cos\phi = R \sin\phi \tag{38B}$$

$$v_n = v_Y \cos\phi + v_x \sin\phi = C + R\cos\phi \tag{39B}$$

so that

$$v_r^2 + (v_n - C)^2 = R^2 \tag{34F}$$

In rotating polar coordinates, the velocity hodograph of an elliptical orbit appears as shown in Figure 3. In general, all conic sections of orbit are defined by the hodograph equations without change, as shown in Figure 4. This polar velocity hodograph has been useful for analysis of the orbital transfer problem (Ref. 2, 3, 6, 7, 8, 9). Some basic mapping relations for the hodograph transformation are presented in Table I.

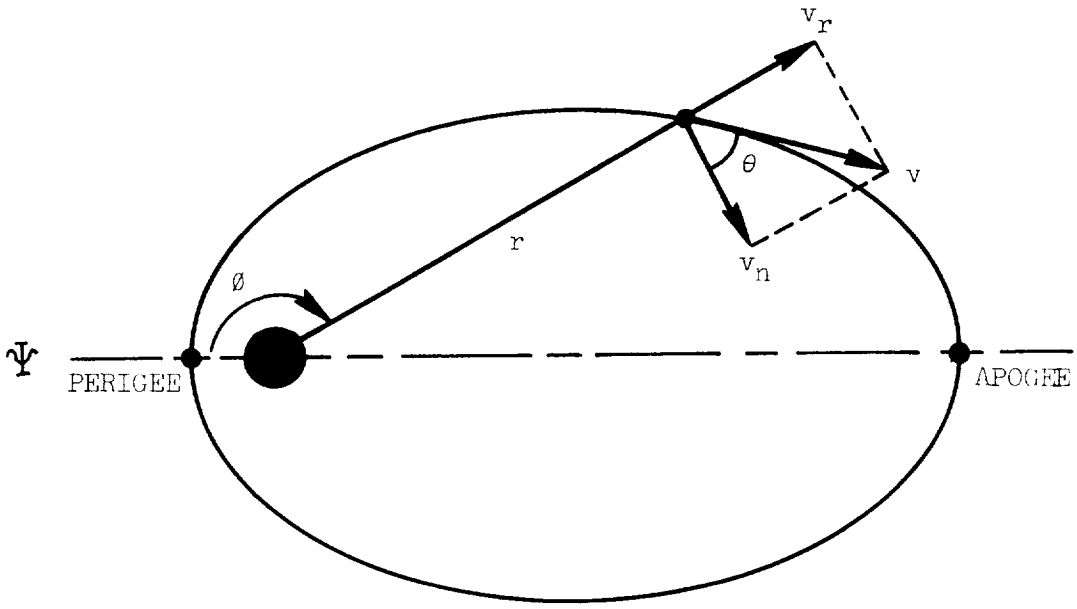

A. ORBIT IN SPACE

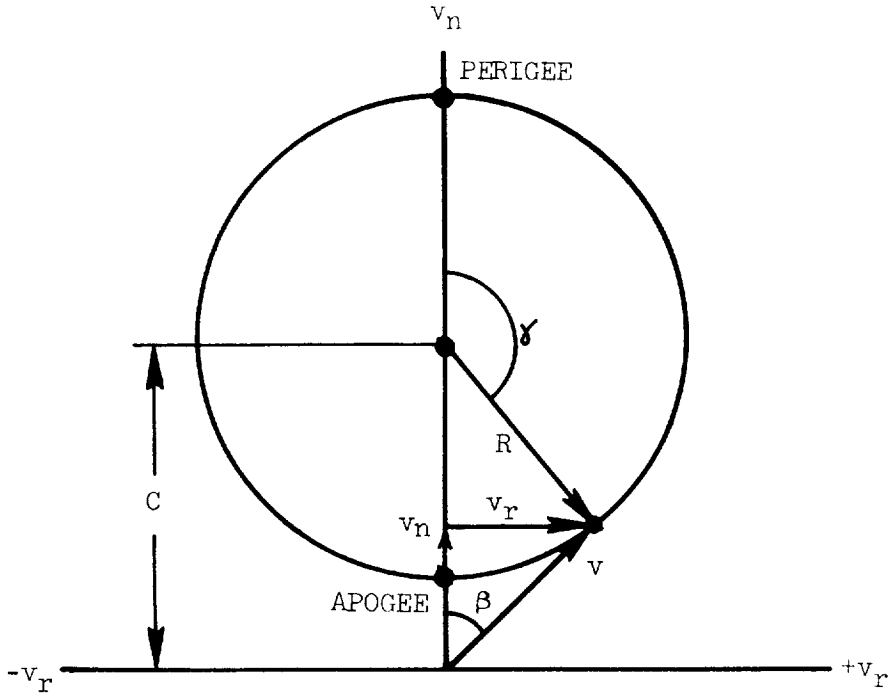

B. ORBIT HODOGRAPH

Fig. 3 Planar Orbit and Its Hodograph

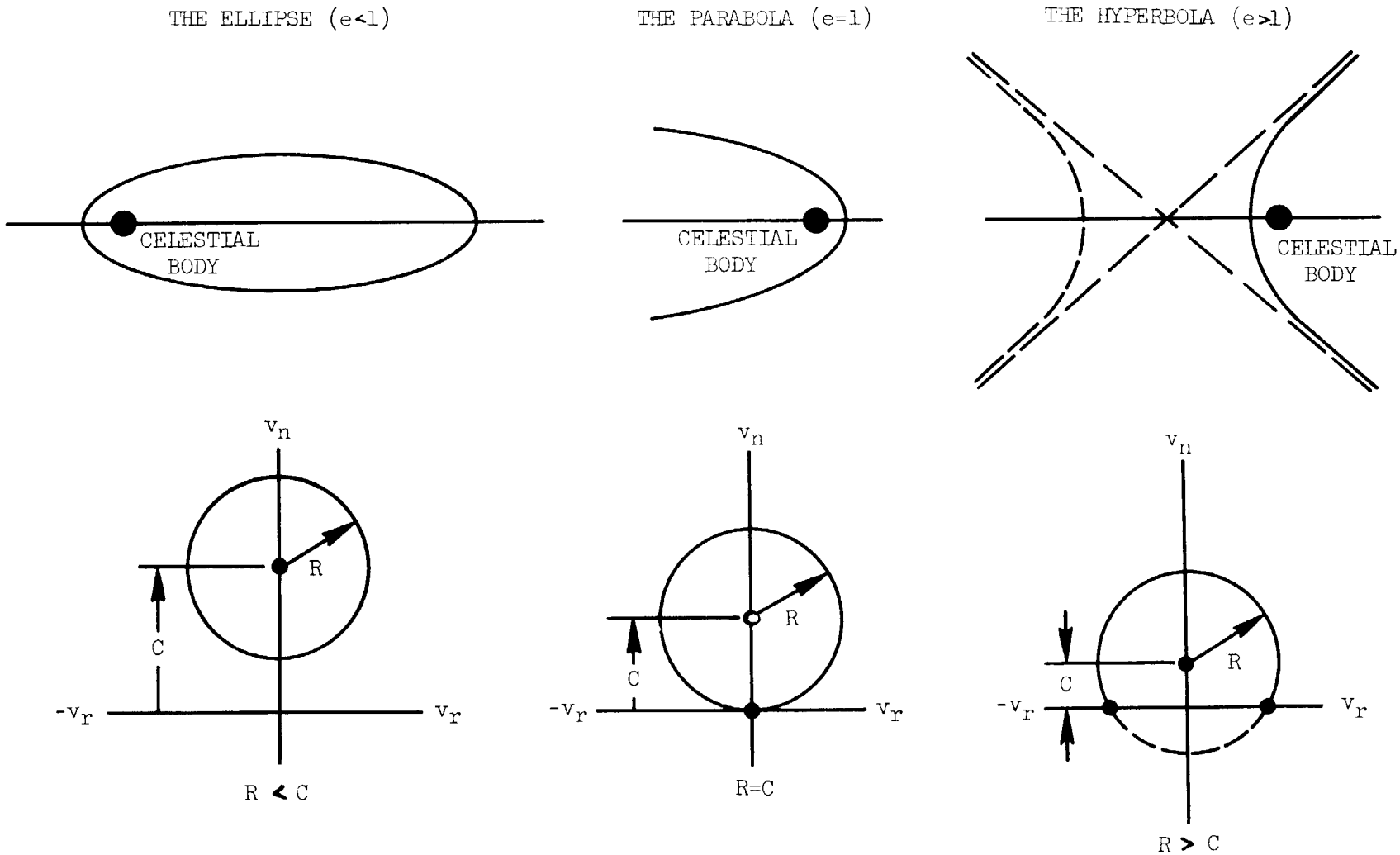

Fig. 4 Polar Velocity Hodograph for the Conic Figures of Orbit

TABLE I

VELOCITY HODOGRAPH TRANSFORMATIONS FOR AN ORBIT

$$C = \frac{\mu}{r v_n} \tag{36}$$

$$R = \sqrt{\frac{2E}{m} + C^2} = \sqrt{2\tilde{E} + C^2} \tag{37}$$

$$v_r = R \sin\phi \tag{38}$$

$$v_n = C + R \cos\phi \tag{39}$$

$$\phi = \gamma \tag{44}$$

$$\theta = \beta \tag{45}$$

$$e = \frac{R}{C} \tag{46}$$

$$a' = \frac{\mu}{C^2 - R^2} \tag{47}$$

$$n = \frac{(C^2 - R^2)^{\frac{3}{2}}}{\mu} \tag{48}$$

$$a'(1 - e^2) = \frac{\mu}{C^2} \tag{49}$$

VI. HODOGRAPH EQUATIONS OF MOTION

The general equations of motion (Eq. 10C and 14C, or 26) are now to be expressed as functions of C,R, ϕ (and the time-derivatives thereof) rather than r, ν (and the time-derivatives thereof). From Equation 38A,

$$\ddot{r} = \dot{R}\sin\phi + R\dot{\phi}\cos\phi, \tag{50}$$

and from Equation 39A,

$$\dot{r}\dot{\nu} + r\ddot{\nu} = \dot{C} + \dot{R}\cos\phi - R\dot{\phi}\sin\phi. \tag{51}$$

Then, from Equation 10C,

$$\Delta a_r = \frac{F_r}{m} = (\dot{R}\sin\phi + R\dot{\phi}\cos\phi) - (C\dot{\nu} + R\dot{\nu}\cos\phi) + C\dot{\nu} \tag{52A}$$

and from Equation 14C,

$$\Delta a_n = \frac{F_\nu}{m} = (\dot{C} + \dot{R}\cos\phi - R\dot{\phi}\sin\phi) + (R\dot{\nu}\sin\phi). \tag{53A}$$

Since

$$\nu = \Psi + \phi, \tag{54}$$

$$\dot{\nu} = \dot{\Psi} + \dot{\phi} \tag{55}$$

so that

$$\Delta a_r = \frac{F_r}{m} = \dot{R}\sin\phi - R\dot{\Psi}\cos\phi \tag{52B}$$

$$\Delta a_n = \frac{F_n}{m} = \dot{C} + \dot{R}\cos\phi + R\dot{\Psi}\sin\phi \tag{53B}$$

respectively. In vector form,

$$\ddot{\bar{r}} = \frac{\bar{F}}{m} = (\dot{R}\sin\phi - R\dot{\Psi}\cos\phi - C\dot{\nu})\bar{T} + (\dot{C} + \dot{R}\cos\phi + R\dot{\Psi}\sin\phi)\bar{J} \tag{56A}$$

or

$$\ddot{\bar{r}} = (\Delta a_r - C\dot{\nu})\bar{T} + (\Delta a_n)\bar{J} \tag{56B}$$

Note that the gravitational attraction provides the $C\dot{\nu}$-term in the $\bar{\imath}$ -direction.

In a rectilinear coordinate system,

$$a_x = a_n \sin\phi - a_r \cos\phi = \dot{C}\sin\phi + R\dot{\Psi} + C\dot{\nu}\cos\phi \tag{57}$$

$$a_Y = a_n \cos\phi + a_r \sin\phi = \dot{R} + \dot{C}\cos\phi - C\dot{\nu}\sin\phi \tag{58}$$

so that

$$(a_x - R\dot{\Psi})^2 + (a_Y - \dot{R})^2 = \dot{C}^2 + (C\dot{\nu})^2 . \tag{59}$$

Conversely, note that

$$a_r = a_Y \sin\phi - a_x \cos\phi = \dot{R}\sin\phi - R\dot{\Psi}\cos\phi - C\dot{\nu} \tag{60}$$

$$a_n = a_Y \cos\phi + a_x \sin\phi = \dot{C} + \dot{R}\cos\phi + R\dot{\Psi}\sin\phi \tag{61}$$

so that

$$(a_r + C\dot{\nu})^2 + (a_n - \dot{C})^2 = (\dot{R})^2 + (R\dot{\Psi})^2 . \tag{62}$$

A. Acceleration Hodograph of an Orbit

As shown in the previous chapter, the velocity hodograph of an orbit is a circle. What can be said about the acceleration hodograph of an orbit?

For the ballistic trajectory, the acceleration due to thrust is zero (i.e., $\Delta a_r = \Delta a_n = 0$) so that Equation 56 reduces to

$$\ddot{\bar{r}} = (-C\dot{\nu})\bar{\imath} \equiv (-C\dot{\phi})\bar{\imath} . \tag{63}$$

In this case, the true anomaly rate $\dot{\phi}$ is identically the radius direction angle rate $\dot{\nu}$, since the apsidal line Ψ (to which the true anomaly is referenced) does not change in the ballistic problem (neglecting oblateness effects, of course). In terms of the acceleration polar scalar,

$$\rho = C\dot{\phi} . \tag{64}$$

However, it can be shown by use of Equation 36 that

$$\dot{\phi} = \left(\frac{C}{\mu}\right) v_n^2 = \frac{C}{\mu}(C + R\cos\phi)^2 \tag{65}$$

so that

$$\rho = \frac{C^2}{\mu}(C + R\cos\phi)^2 \tag{64B}$$

or

$$\rho = \frac{C^4}{\mu}(1 + e\cos\phi)^2 \tag{64C}$$

This equation is recognizable as a form of Pascal's limaçon (Ref. 19, 20) defined by

$$P = c + d\cos\phi \tag{66}$$

The limaçon is described, and some properties of the acceleration hodograph are derived from the basic form of the limaçon, in Appendix B. Consequently, the acceleration hodograph can also be used to represent all conic sections of orbit, as shown in Figure 5. Some basic mapping relations for the accceleration hodograph transformation are shown in Table II. However, the simpler hodograph figure and mapping relations shown in Figure 6 are more amenable to study and interpretation of the acceleration hodograph characteristics.

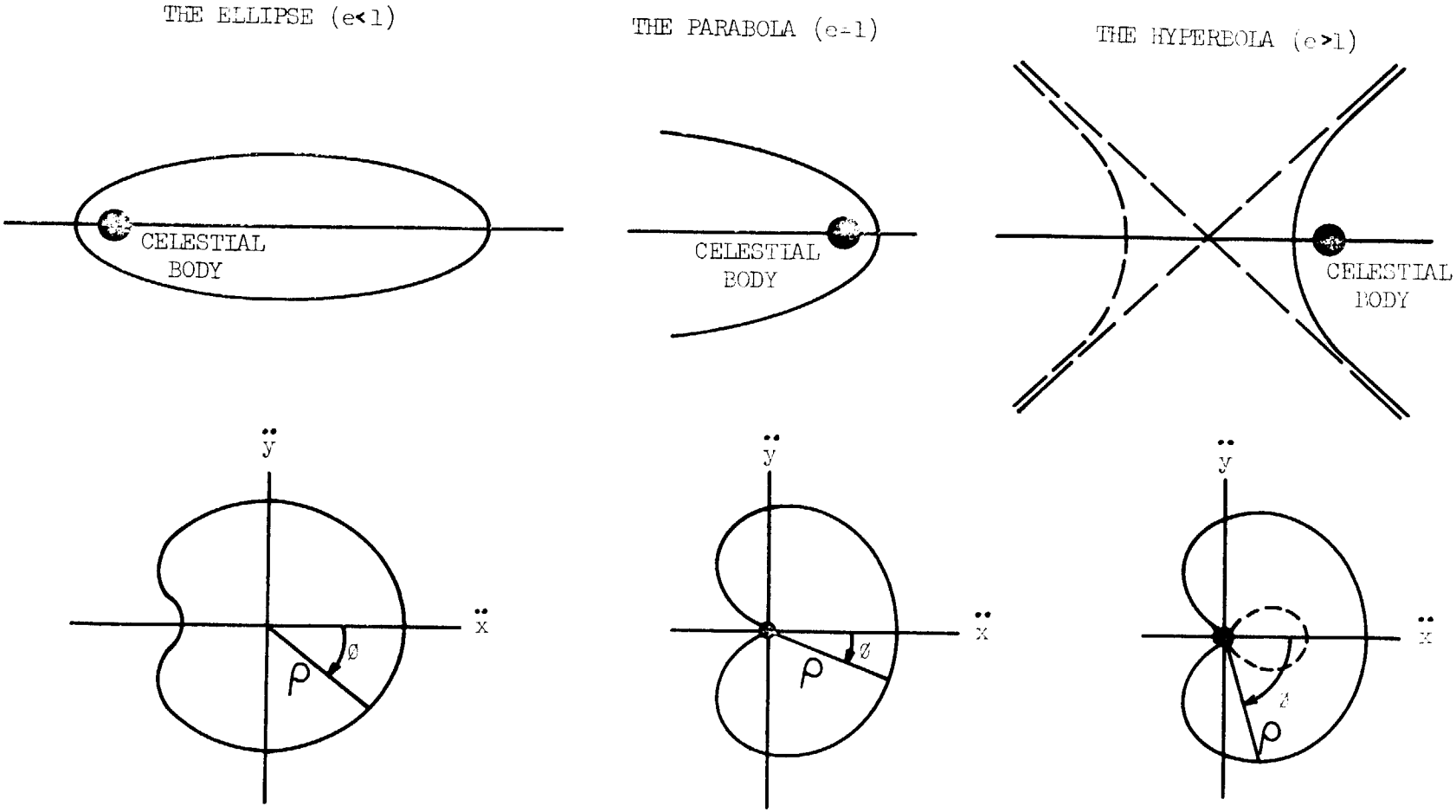

Fig. 5 Acceleration Limaçon for the Conic Figures of Orbit

TABLE II

ACCELERATION HODOGRAPH TRANSFORMATIONS FOR AN ORBIT

$$\rho = C\,\dot{\phi} \tag{64}$$

$$\dot{\phi} = \left(\frac{C}{\mu}\right) v_n^2 \tag{65}$$

$$r = \sqrt{\frac{\mu}{\rho}} \tag{67}$$

$$C v_n = \sqrt{\mu \rho} \tag{68}$$

$$C v_r = \frac{\sqrt{\mu \rho}}{2} \tan\theta' \tag{69}$$

$$\frac{v_r}{v_n} = \frac{1 - u \tan\phi}{2(u + \tan\phi)} \tag{70}$$

$$\phi = \arctan\left[\frac{1 - u \tan\theta'}{u + \tan\theta'}\right] \tag{71}$$

$$e = (2 \sin\phi \cot\theta' - \cos\phi)^{-1} \tag{72}$$

$$a' = \frac{2(2 - \cot\phi \tan\theta')}{4 \csc^2\phi - (\tan\theta' + 2\cot\phi)^2} \sqrt{\frac{\mu}{\rho}} \tag{73}$$

$$p = \frac{2}{2 - \cot\phi \tan\theta'} \sqrt{\frac{\mu}{\rho}} \tag{74}$$

$$C = (\mu\rho)^{\frac{1}{4}} \left(1 - \frac{\cot\phi \tan\theta'}{2}\right)^{\frac{1}{2}} \tag{75}$$

$$R = (\mu\rho)^{\frac{1}{4}} \frac{\tan\theta' \csc\phi}{\left[2(2 - \cot\phi \tan\theta')\right]^{\frac{1}{2}}} \tag{76}$$

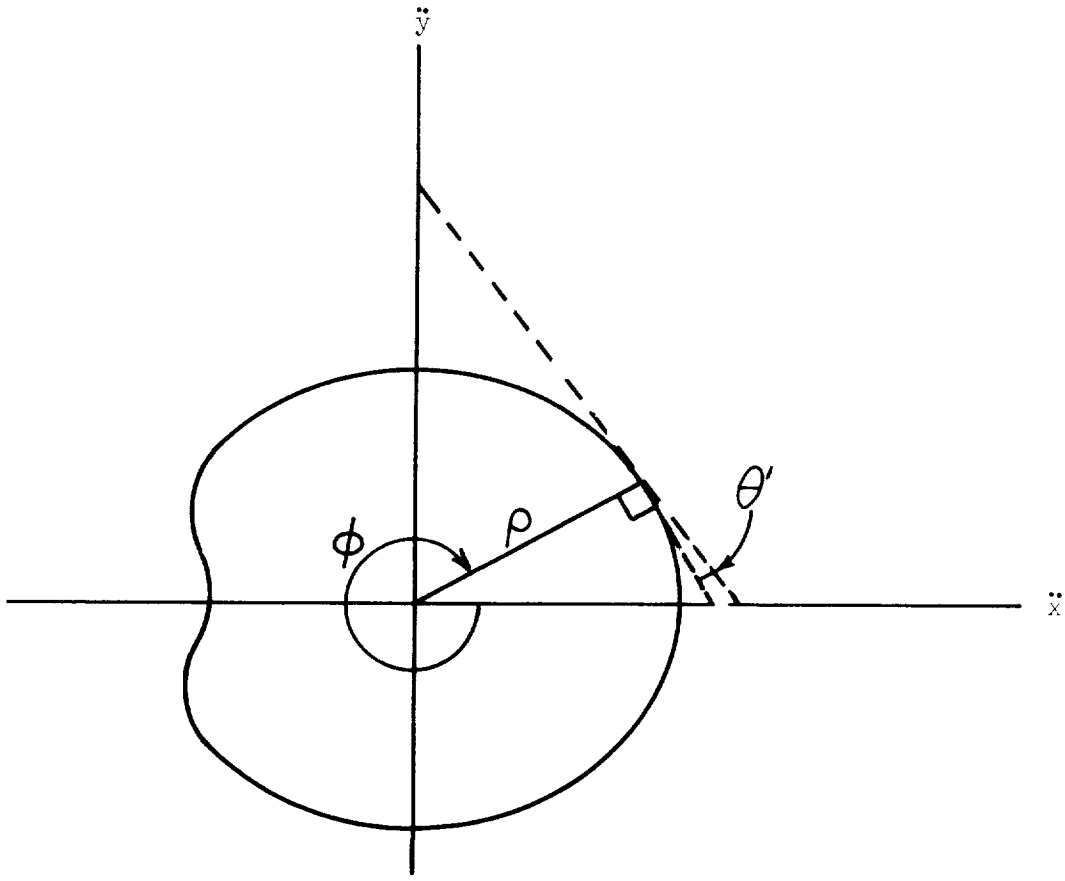

ACCELERATION PLANE ⟶ SPACE PLANE	ACCELERATION PLANE ⟶ VELOCITY PLANE	
$\rho = \frac{\mu}{r^2} = c\dot{\phi}$	$\rho = \frac{(C v_n)^2}{\mu}$	(77)
$\tan\theta' = 2\tan\theta$	$\tan\theta' = 2\left(\frac{v_r}{v_n}\right)$	(78)

Fig. 6 Acceleration Hodograph Summary

B Variation of the Direction Angle Reference

In the basic definition of the hodograph and referring to Figure 1, the angle between the radius vector line (defined by $\bar{N}$) and the reference line fixed in inertial space is the direction angle ν. The hodograph is only defined for a fixed reference line. For orbits, the apsidal line directed to perigee passage (defined by Ψ) may be selected as the most convenient reference line. In general, however, this apsidal line will change its orientation in inertial space whenever thrust is applied. Consequently, the hodograph parameters are only defined, in the case of a continuous thrust program, for a continuum (in time or space) of instantaneous orbital hodographs with the parameters C, R, and Ψ as functions of time. The apsidal line orientation Ψ is seen to be a function of $\dot{C}$ and $\dot{R}$ upon consideration of the definitive equation for the parameter C of an instantaneous hodograph:

$$C = \frac{\mu}{rv_n} \tag{36}$$

Then

$$r = \mu(C^2 + CR\cos\phi)^{-1} \tag{79}$$

$$\dot{r} = -\mu(C^2 + CR\cos\phi)^{-2}(2C\dot{C} + \dot{C}R\cos\phi + C\dot{R}\cos\phi - CR\dot{\phi}\sin\phi) \tag{80A}$$

or

$$v_r = -\mu(Cv_n)^{-2}(C\dot{C} + \dot{C}v_n + C\dot{R}\cos\phi - Cv_r\dot{\phi}). \tag{80B}$$

But $$\dot{\phi} = \dot{\nu} - \dot{\Psi} \tag{81}$$

so that

$$(Cv_n)^2 v_r = -\mu\left[C\dot{C} + \dot{C}v_n + C\dot{R}\left(\frac{v_n - C}{R}\right) - Cv_r\dot{\nu} + Cv_r\dot{\Psi}\right] \tag{82A}$$

Since, by Equation 36,

$$C\dot{\nu} = \frac{(Cv_n)^2}{\mu} \tag{83}$$

then $$(Cv_n)^2 v_r = +(Cv_n)^2 v_r - \mu\left[C\dot{C} + \dot{C}v_n + C\dot{R}\left(\frac{v_n - C}{R}\right) + Cv_r\dot{\Psi}\right] \tag{82B}$$

or

$$CR\dot{C} + R\dot{C}v_n + C\dot{R}v_n - C^2\dot{R} + CRv_r\dot{\Psi} = 0 \tag{84}$$

Therefore

$$-\dot{\Psi} = \frac{\dot{C}}{C}\left(\frac{v_n + C}{v_r}\right) + \frac{\dot{R}}{R}\left(\frac{v_n - C}{v_r}\right) \tag{85A}$$

or

$$-\dot{\Psi} = \frac{\dot{C}}{C}\left(\frac{2C + R\cos\phi}{R\sin\phi}\right) + \frac{\dot{R}}{R}(\cot\phi) \tag{86B}$$

C. Transformation of Parameters from the Time-Domain

The hodograph equations of motion were previously defined by constants, and by parameters which are time-dependent. However, if these parameters are constrained so that they are functions of space coordinates rather than time, the parameters and the consequent equations of motions may be transformed from the time domain of formulation. For example, assume that C and R are functions of the instantaneous true anomaly ϕ, by suitable constraint of the thrust vector magnitude and direction. This condition could be provided by an idealized closed-loop control in response to an inertial sensor subsystem and guidance controller. Then

$$\dot{C} = \frac{dC}{dt} = \frac{dC}{d\phi}\frac{d\phi}{dt} \tag{87A}$$

so that

$$\dot{C} = C_\phi\dot{\phi} \tag{87B}$$

and

$$\dot{R} = \frac{dR}{dt} = \frac{dR}{d\phi}\frac{d\phi}{dt} \tag{88A}$$

so that

$$\dot{R} = R_\phi\dot{\phi} \tag{88B}$$

Also

$$\dot{\phi} = \frac{\dot{C}}{C_\phi} = \frac{\dot{R}}{R_\phi} = \frac{C}{\mu}(C + R\cos\phi)^2 \tag{89}$$

Utilizing these transformed parameter variables (C_ϕ, R_ϕ), the hodograph equations of motion may be directly transformed.

This change in the independent variable from time to a space-coordinate suggests itself as a potential technique for synthesis and analysis of space trajectories resulting from closed-loop guidance and control.

VII. LUNAR LANDING PROBLEM

The hodograph transformation will be applied to a thrust program class of immediate interest to the Langley Research Center, for possible use in the lunar descent and landing problem of the manned Apollo mission. In particular, a closed-form (or analytic) solution was desired. Although such solution has not been attained, the resulting equations should enable considerable insight into and understanding of the characteristic performance of this trajectory class.

In this problem, the magnitude of the thrust vector is always constant, while the thrust vector is always directed opposite to the velocity vector. The rocket fuel mass flow rate is constant, so that

$$m = m_0 + kt \quad , \tag{19C}$$

as shown previously.

As noted in Appendix A, the thrust program would be applied at the perigee passage on an elliptical orbit about the moon, as shown in Figure 7.

A. Basic Hodograph Equations of Motion

The thrust and velocity vectors are related as shown in Figure 8.

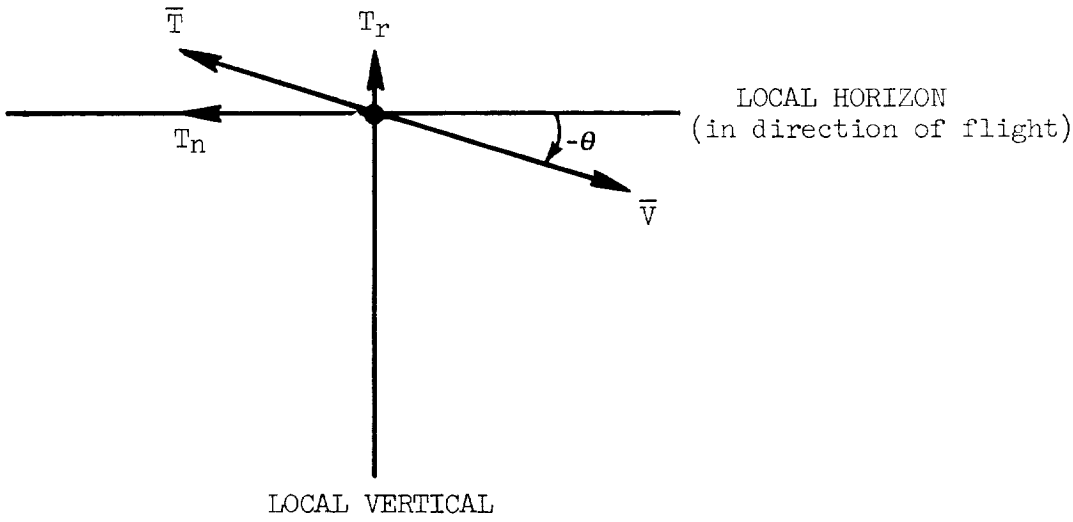

Fig. 8 Vector Definition of the Lunar Landing Thrust Program

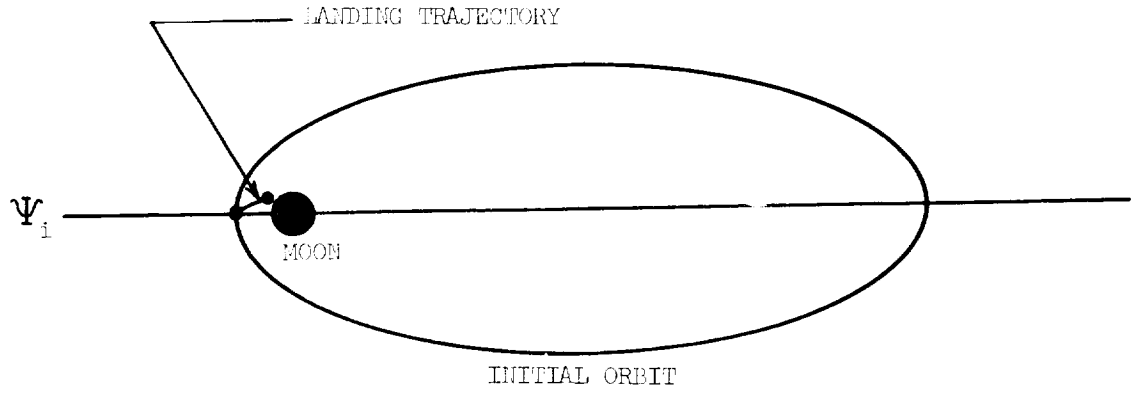

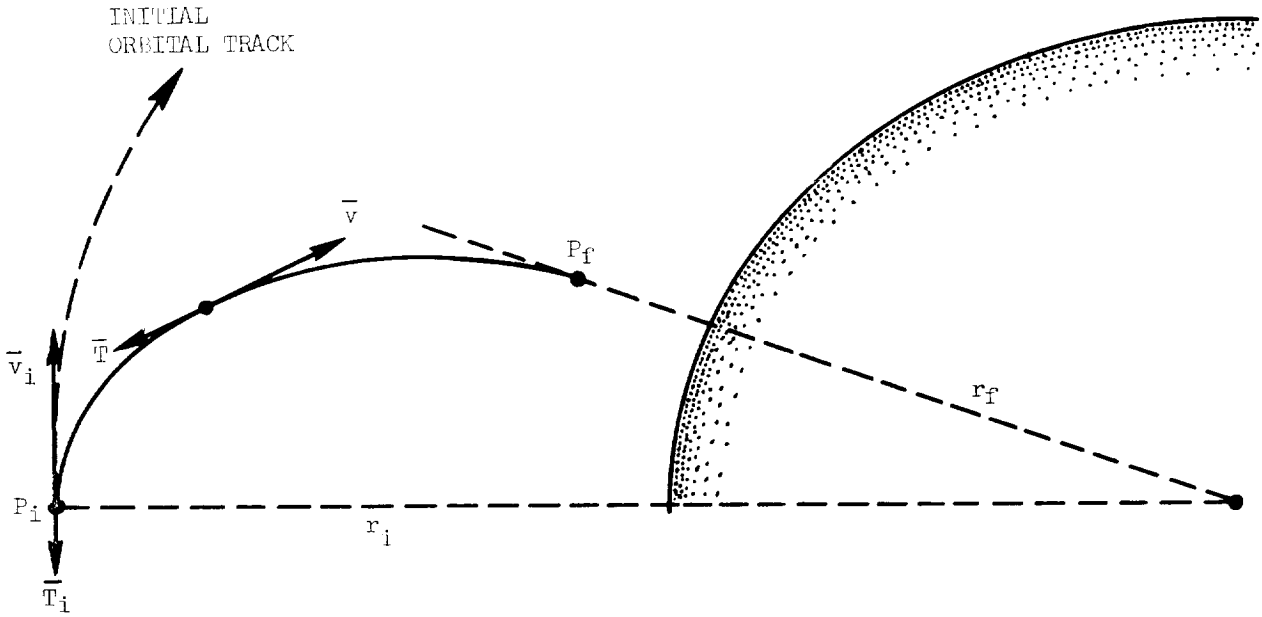

Fig. 7 The Lunar Landing Trajectory

$$\Delta a_r = -\frac{T_r}{m} = -\frac{T}{m}\sin\theta = -\left(\frac{T}{m}\right)\frac{v_r}{v} \tag{90A}$$

$$\Delta a_n = -\frac{T_n}{m} = -\frac{T}{m}\cos\theta = -\left(\frac{T}{m}\right)\frac{v_n}{v} \tag{91A}$$

Consequently, by use of Equations 52B and 53B,

$$\Delta a_r = -\left(\frac{T}{m}\right)\frac{v_r}{v} = \dot{R}\sin\phi - R\dot{\Psi}\cos\phi \tag{90B}$$

or

$$-\left(\frac{T}{m}\right)\frac{R\sin\phi}{v} = \dot{R}\sin\phi - R\dot{\Psi}\cos\phi \quad , \tag{90C}$$

and

$$\Delta a_n = -\left(\frac{T}{m}\right)\frac{v_n}{v} = \dot{C} + \dot{R}\cos\phi + R\dot{\Psi}\sin\phi \tag{91B}$$

or

$$-\left(\frac{T}{m}\right)\frac{C + R\cos\phi}{v} = \dot{C} + \dot{R}\cos\phi + R\dot{\Psi}\sin\phi \; . \tag{91C}$$

Therefore

$$-\frac{T}{mv} = \frac{\dot{R}\sin\phi - R\dot{\Psi}\cos\phi}{R\sin\phi} \tag{92A}$$

and

$$-\frac{T}{mv} = \frac{\dot{C} + \dot{R}\cos\phi + R\dot{\Psi}\sin\phi}{C + R\cos\phi} \tag{92B}$$

so that, upon combining Equations 92A and 92B,

$$\dot{R}C\sin\phi + \cancel{\dot{R}B\sin\phi\cos\phi} - CR\dot{\Psi}\cos\phi - R^2\dot{\Psi}\cos^2\phi$$
$$= \dot{C}R\sin\phi + \cancel{\dot{R}B\sin\phi\cos\phi} + R^2\dot{\Psi}\sin^2\phi \qquad (93A)$$

$$(\dot{R}C - \dot{C}R)\sin\phi - R\dot{\Psi}(R + C\cos\phi) = 0 \qquad (93B)$$

$$\dot{\Psi} = \frac{\left(\frac{\dot{R}}{R} - \frac{\dot{C}}{C}\right)\sin\phi}{\left(\frac{R}{C}\right) + \cos\phi} \qquad (93C)$$

Consequently, substituting Equation 93C for $\dot{\Psi}$ in Equation 90C,

$$-\left(\frac{T}{mv}\right)R\sin\phi = \frac{\dot{R}\sin\phi(R + C\cos\phi) - \sin\phi\cos\phi(\dot{R}C - \dot{C}R)}{R + C\cos\phi} \qquad (90D)$$

$$-\left(\frac{T}{mv}\right)R = \frac{\dot{R}(R + \cancel{C\cos\phi} - \cancel{C\cos\phi}) + \dot{C}(R\cos\phi)}{R + C\cos\phi} \qquad (90E)$$

$$-\frac{T}{mv} = \frac{\dot{R} + \dot{C}\cos\phi}{R + C\cos\phi} \qquad (90F)$$

The same result (i.e., Eq. 90F) would be obtained upon substitution of Equation 93C for $\ddot{\psi}$ in Equation 91C.

The general expression (Eq. 86B) for $\dot{\Psi}$ may be equated with the special expression (Eq. 93C) to obtain

$$\frac{\left(\frac{\dot{R}}{R} - \frac{\dot{C}}{C}\right)\sin\phi}{\left(\frac{R}{C}\right) + \cos\phi} = -\frac{\dot{C}(2C + R\cos\phi)}{CR\sin\phi} - \frac{\dot{R}\cos\phi}{R\sin\phi} \qquad (94A)$$

Reduction of Equation 94A results in

$$\frac{\dot{C}}{C} = -\frac{\dot{R}}{R+2C\cos\phi} \tag{94B}$$

The combined use of Equations 90F and 94B provides

$$\frac{T}{mv} = \frac{\dot{C}}{C} \tag{95A}$$

The use of Equation 94B with Equation 93C provides

$$\dot{\Psi} = -\dot{C}\left(\frac{2\sin\phi}{R}\right) \tag{93D}$$

Equations 93-95 comprise the basic hodograph equations of motion for the lunar landing problem. These equations, together with various potentially useful auxiliary equations which were obtained from them, are summarized in Table III. In addition, the following general equations of the basic hodograph theory are useful:

$$\dot{\nu} = \dot{\Psi} + \dot{\phi} \tag{55}$$

$$\dot{\nu} = \frac{C}{\mu}(C+R\cos\phi)^2 \tag{100}$$

$$v^2 = R^2 + C^2 + 2RC\cos\phi \tag{101}$$

Equation 95A or 95B in Table III provides the following vector equation for the lunar landing problem:

$$\overline{\Delta a} = -\left|\frac{\dot{C}}{C}\right|(v_r\bar{i} + v_n\bar{j}) \tag{102}$$

The trigonometric character of the equations in Table III enables a simple geometric construction which presents these hodograph equations of motion, at any given instant of time. The definitive triangles are shown in Figure 9, with all equation terms suitably identified.

The hodograph equations of motion may be treated in two different ways, to obtain trajectory solutions:

$$\frac{T}{mv} = \frac{\dot{C}}{C} = -\frac{\dot{R}}{R+2C\cos\phi} = -\frac{\dot{R}+\dot{C}\cos\phi}{R+C\cos\phi} \qquad (95A;95D;95F)$$

$$\dot{\Psi} = -\dot{C}\left(\frac{2\sin\phi}{R}\right) \qquad (93J)$$

or

$$\dot{\Psi} = \left(\frac{\dot{R}}{R} - \frac{\dot{C}}{C}\right)\frac{C\sin\phi}{R+C\cos\phi} = \left(\frac{\dot{R}}{R} - \frac{\dot{C}}{C}\right)\frac{v_x}{v_y} = \left(\frac{\dot{R}}{R} - \frac{\dot{C}}{C}\right)\tan(\phi-\theta) \qquad (93M)$$

or

$$\dot{\Psi} = \left(\frac{\dot{R}}{R} + \frac{\dot{C}}{C}\right)\tan\phi \qquad (93F)$$

$$\cos\phi = -\frac{1}{2}\left(\frac{\dot{R}}{\dot{C}} + \frac{R}{C}\right) \qquad (96)$$

$$\left(\frac{T}{m}\right)v = \dot{C}C - \dot{R}R = \left(\frac{\dot{C}}{C}\right)v^2 \qquad (97;95E)$$

$$\left(\frac{T}{m}\right)^2 = \left(\frac{\dot{C}v}{C}\right)^2 = \dot{R}^2 + \dot{C}^2 + 2\dot{R}\dot{C}\cos\phi \qquad (95C;98A)$$

or

$$\left(\frac{T}{m}\right)^2 = \frac{\dot{C}}{C}\left(C\dot{C} - R\dot{R}\right) \qquad (98B)$$

$$R\dot{R} = \frac{\dot{C}}{C}\left(C^2 - v^2\right) \qquad (99)$$

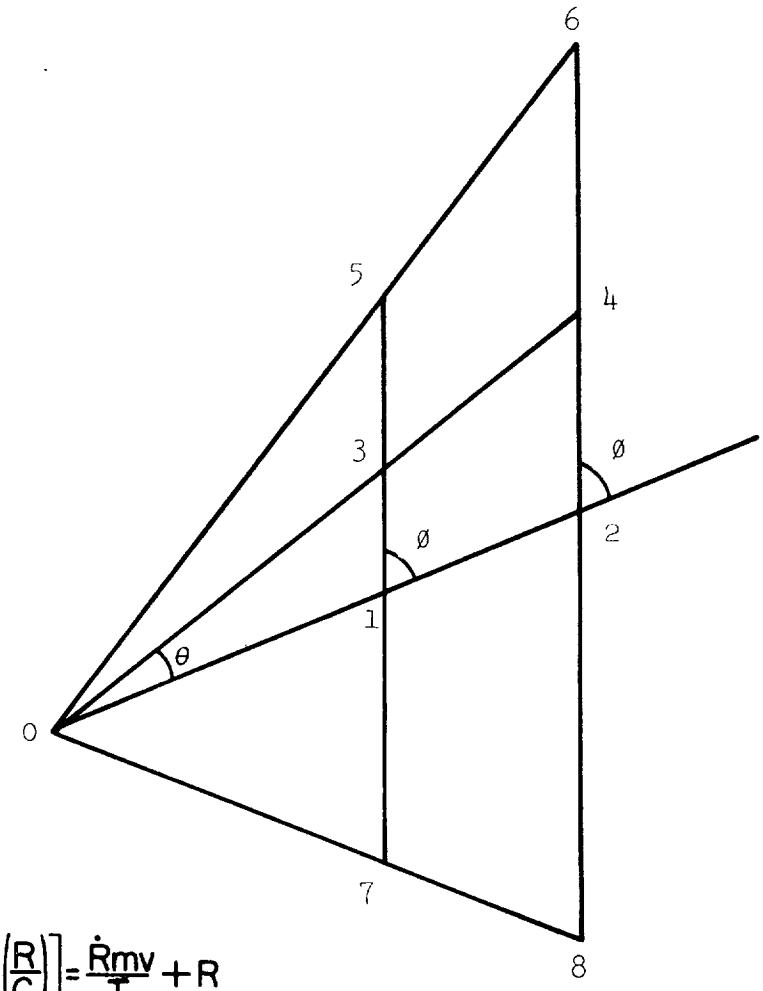

01 = $\dot{C}$

02 = C

15 = $\dot{R}$

24 = R

46 = $2C\cos\phi = \frac{mv}{T}\left[\dot{R} + \dot{C}\left(\frac{R}{C}\right)\right] = \frac{\dot{R}mv}{T} + R$

03 = $\frac{I}{m}$

04 = v

28 = $R + 2C(\cos\phi - \sin\phi) = \frac{C}{C}(R\dot{\Psi} - \dot{R})$

17 = $R\dot{\Psi} - \dot{R}$

Fig. 9 Geometric Representation of the LLP Hodograph Equations of Motion

1. Integration, to obtain the continuum of instantaneous hodographs as a function of time.

2. Generation of the hodograph (or trajectory mapping) in the "acceleration plane."

With integration, only one integration is required, since the instantaneous hodograph completely defines both the velocity and space coordinates. While analytic integration to obtain closed-form solution is highly desirable, machine integration is currently most common in general synthesis work. In this latter case, programming and machine solution are expedited with hodograph equations, due to the need for only one integration rather than the two integrations with the usual equations of motion.

If a general formulation of hodograph generating theory (or differential geometry) were available, the direct use of the hodograph equations would be obvious. However, in the absence of such general theory, the hodograph equations can only be studied, relative to possible generating techniques, by the elimination of time as a variable. Consequently, the hodograph equations must be transformed from the time-domain to the "acceleration space plane."

B. Transformation of Equations from the Time-Domain

Let us consider the hodograph equations in Table III. All equations in which mass (m) does not appear can be expressed as differential equations in C, R, and ϕ (or ν), as presented in Table IV.

TABLE IV

TIME-FREE HODOGRAPH EQUATIONS OF MOTION
FOR THE LUNAR LANDING PROBLEM

$$\frac{dC}{C} = -\frac{dR}{R+2C\cos\phi} = -\frac{dR+dC(\cos\phi)}{R+C\cos\phi} \tag{103}$$

$$d\Psi = -dC\left(\frac{2\sin\phi}{R}\right) \tag{104A}$$

or

$$d\Psi = \left(\frac{dR}{R} - \frac{dC}{C}\right)\frac{C\sin\phi}{R+C\cos\phi} = \left(\frac{dR}{R} - \frac{dC}{C}\right)\frac{v_x}{v_y} \tag{104B}$$

or

$$d\Psi = \left(\frac{dR}{R} + \frac{dC}{C}\right)\tan\phi \tag{104C}$$

$$\cos\phi = -\frac{1}{2}\left(\frac{dR}{dC} + \frac{R}{C}\right) \tag{105}$$

$$CdC - RdR = \left(\frac{v^2}{C}\right)dC \tag{106}$$

$$\left(\frac{vdC}{C}\right)^2 = (dR)^2 + (dC)^2 + 2(dR)(dC)\cos\phi \tag{107}$$

In this case, it is most convenient to use ϕ (or ν) as the independent variable, rather than C, R, or ψ, by use of Equations 55, 100 and 101. By use of the equations in Table IV, the following pair of equations, which contain only the differentials for C, R and ϕ, are obtained:

$$dC\left[(C+R\cos\phi)^2\sqrt{C^2+R^2+2CR\cos\phi}+\frac{\left(\frac{2\mu T}{m}\right)\sin\phi}{R}\right]=\left(\frac{\mu T}{m}\right)d\phi \tag{108}$$

$$dR\left[\frac{CR(C+R\cos\phi)^2\sqrt{C^2+R^2+2CR\cos\phi}+\left[\frac{2\mu TC}{m}\right]\sin\phi}{R(R+2C\cos\phi)}\right]=-\left(\frac{\mu T}{m}\right)d\phi \tag{109}$$

As shown by Equation 100, mass is inextricably a function of time in this lunar landing problem, since the mass variation is so defined. However, note that this time relation would not occur if mass variation were defined, or controlled, as a function of space, velocity, or acceleration coordinates. As far as is known, such controlled variation of mass has not been studied. If such mass control as a function of coordinates (rather than time) enables closed-form solutions to be obtained thereby, consequent thrust programs (or control laws) might prove most desirable as a result of a high order of prediction and repeatability.

C. Orbital Energy Relations

In the lunar landing problem, the orbital energy equation and conditions may provide additional analytic relations, or physical understanding of the trajectory synthesis. In Reference 4, an orbital energy diagram was developed in terms of the hodograph parameters. It was shown that orbits of specified specific energy (E) and of specified eccentricity were uniquely defined by straight lines on this energy diagram.

With thrust application, the orbital energy is obviously changed. In ballistic flight, the vis viva integral provides

$$v^2=\mu\left(\frac{2}{r}-\frac{1}{a'}\right) \tag{110}$$

so that

$$v\dot{v}_b=-\frac{\mu\dot{r}}{r^2} \tag{111}$$

However, the specific energy equation is

$$\tilde{E} = \frac{v^2}{2} - \frac{\mu}{r} \tag{112}$$

so that

$$\dot{\tilde{E}} = v\dot{v} + \frac{\mu \dot{r}}{r^2} \tag{113A}$$

But

$$v\dot{v} = v(\dot{v}_b + \dot{v}_p) \tag{114}$$

so that, by use of Equations 111 and 114,

$$\dot{\tilde{E}} = v\dot{v} - \left(-\frac{\mu \dot{r}}{r^2}\right) = v\dot{v} - v\dot{v}_b = v\dot{v}_p \tag{113B}$$

Since

$$\dot{v}_p = -\frac{T}{m} \tag{115}$$

then

$$\dot{\tilde{E}} = -\left(\frac{T}{m}\right) v \tag{113C}$$

or

$$\dot{\tilde{E}} = R\dot{R} - C\dot{C} = -\left(\frac{\dot{C}}{C}\right) v^2 \tag{113D;113E}$$

Also, the total acceleration may be expressed, as follows:

$$\dot{v} = -\left[\frac{T}{m} + \frac{\mu}{r^2}\left(\frac{v_r}{v}\right)\right] = -\left[\frac{T}{m} + C\dot{\nu}\sin\theta\right] \tag{116A;116B}$$

At this point, an interesting energy relation is noted, which eliminates time in explicit form from the energy variation equation. By definition,

$$\tilde{E} = \frac{E}{m} \tag{117}$$

so that

$$\dot{\tilde{E}} = \frac{\dot{E}}{m} - \frac{E\dot{m}}{m^2} \tag{113F}$$

Consequently,

$$\frac{\dot{E}}{m} - \frac{E\dot{m}}{m^2} = -\left(\frac{T}{m}\right)\dot{s} \tag{113G}$$

so that

$$\frac{dE}{E} = \frac{dm}{m} - \left(\frac{T}{E}\right)ds \tag{118}$$

If the term $\left(\frac{T}{E}\right)$ were constant or a function of path length (s) only, then an integral relation between E, m, and s would be available. At this time, no knowledge of such properties of $\left(\frac{T}{E}\right)$ are known. Also, according to Equation 113C, an integral relation between $\tilde{E}$ and s would be available if the term $\left(\frac{T}{m}\right)$ were constant or a function of path length only. This condition and resulting integral relation were used in References 21 and 22.

D. Machine Solution

When it became apparent that analytic solution would not be attained, at least not at this time, machine solution was obtained by use of an IBM 7090 and a Philco 2000 (Transac) computer. Although such machine computation was not specified in the research contract, machine solution appeared most desirable prior to completion of this initial study effort. While the machine solutions can often provide significant clues to analytical techniques of solution, the programming characteristics of the hodograph equations could also be evaluated cursorily. As noted previously, machine programming of the hodograph equations for solution requires only one integration, while the usual equations of motion (with space coordinates as variables) require two integrations. Consequently, the programming was found to be simpler and to require less machine capacity (or logic).

Machine solution based upon the classical equations of motion was not obtained at United Aircraft. Consequently, sets of data points for such solution were obtained from the Langley Research Center for relative evaluation and solution check. At this point, a basic difference between the two machine programs is noted. In the NASA program, a variable time interval for computation was provided; in the UA hodograph program, a fixed time interval for computation was used. The use of a fixed time interval enabled appraisal of the effects of the variation of such time intervals upon the solution accuracy. For example, the change in relative apparent difference between hodograph equation solution and classical equation solution with change in the time interval of integration, is shown in Figures 10 and 11 for radius (r) and velocity (v). The relative apparent difference (in percent) of the variable is defined as the ratio of the difference in observed values to the average of those observed values at a given trajectory time.

As shown by Figures 10 and 11, reduction of the integration interval improves the computation accuracy greatly in the terminal phase of the trajectory. However, the total solution time for the trajectory run was about 5 minutes for 0.01 seconds integration interval, and about 35-40 minutes for 0.002 seconds integration interval. The solution time would be a critical consideration in real-time solution for inflight operations were desired. That is, if the solution time were equal to or shorter than the real trajectory time, then the actual trajectory could be monitored by an astronaut operator or by a closed-loop system of thrust correction control, to "fly the trajectory wire." Consequently, if the fixed integration interval of 0.01 seconds did not provide required trajectory solution accuracy, the variable integration time interval (as used in the NASA program) or an analytic solution scheme would be required for such real-time applications.

Prior to machine computation, it was apparent, upon reference to the general hodograph equations for an orbit (Table I) or the lunar landing problem equations (Table III), that the terminal point of the specified lunar landing problem defines an orbit which is indeterminate in the hodograph transformation. At the terminal point of the trajectory, the velocity is zero and the thrust is discontinued. Then the terminal orbit is a straight line from the terminal point (or "apogee") to the gravitational center (or "perigee") and such a path lies on a radius from the gravitational center, with zero angular momentum. Then $C \rightarrow \infty$ (Eq. 36 or 95A) and $R \rightarrow \infty$ (Eq. 37 or 94C).

Remembering that the hodograph transformation regularizes all points in the region of solution for real orbits (i.e., nonzero velocity and angular momentum), it is clear that the transformation has a singular point of solution for this class of "orbit" which passes through the attracting center. Nevertheless, the machine solution from the hodograph equation program shows excellent correlation with the solution from the classical equation program, until about 280 seconds (e.g., see Fig. 10). Note that the computing errors implicit in the machine programming and solution of

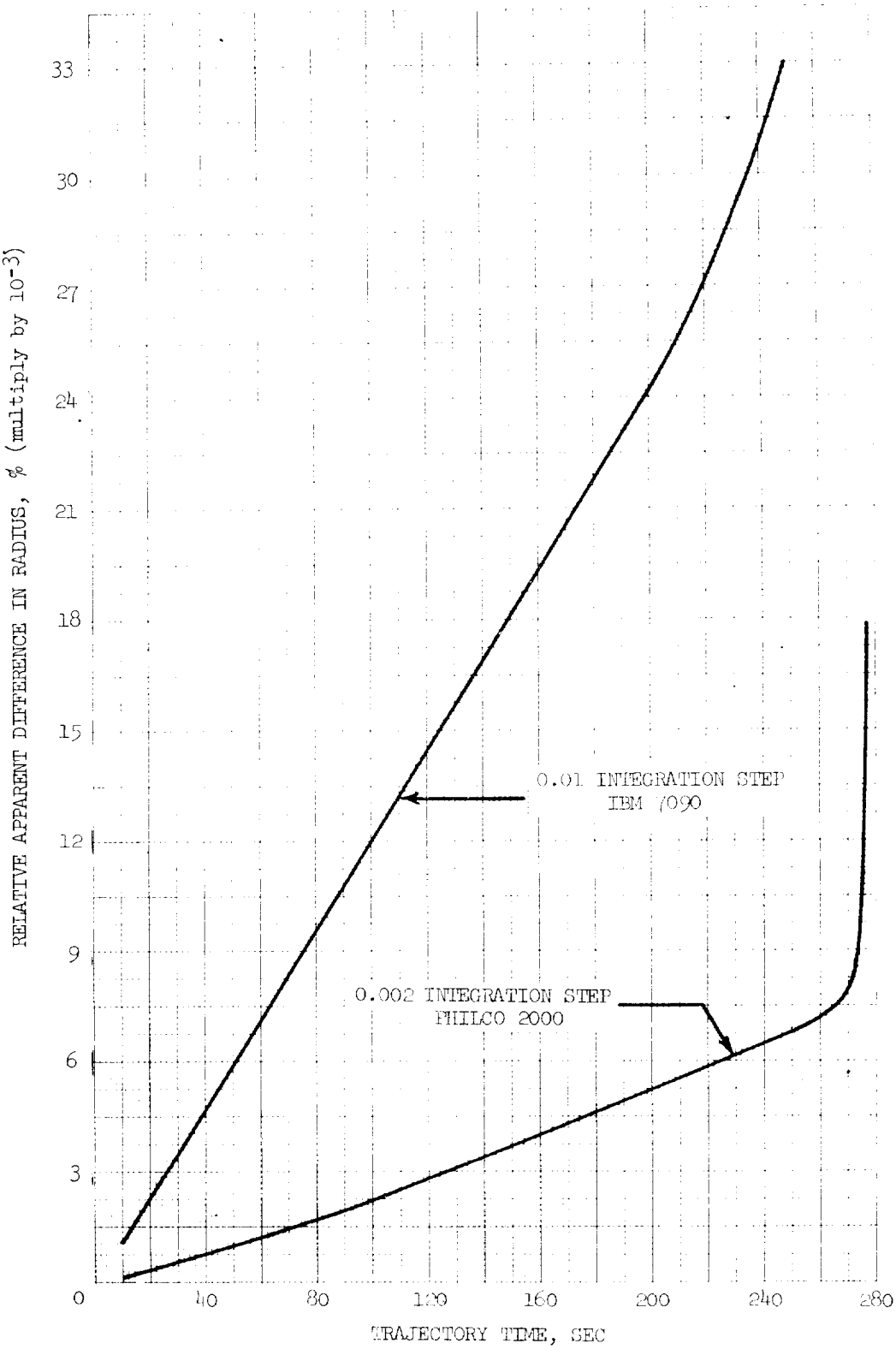

Fig. 10 Influence of Integration Upon Apparent Radius Error

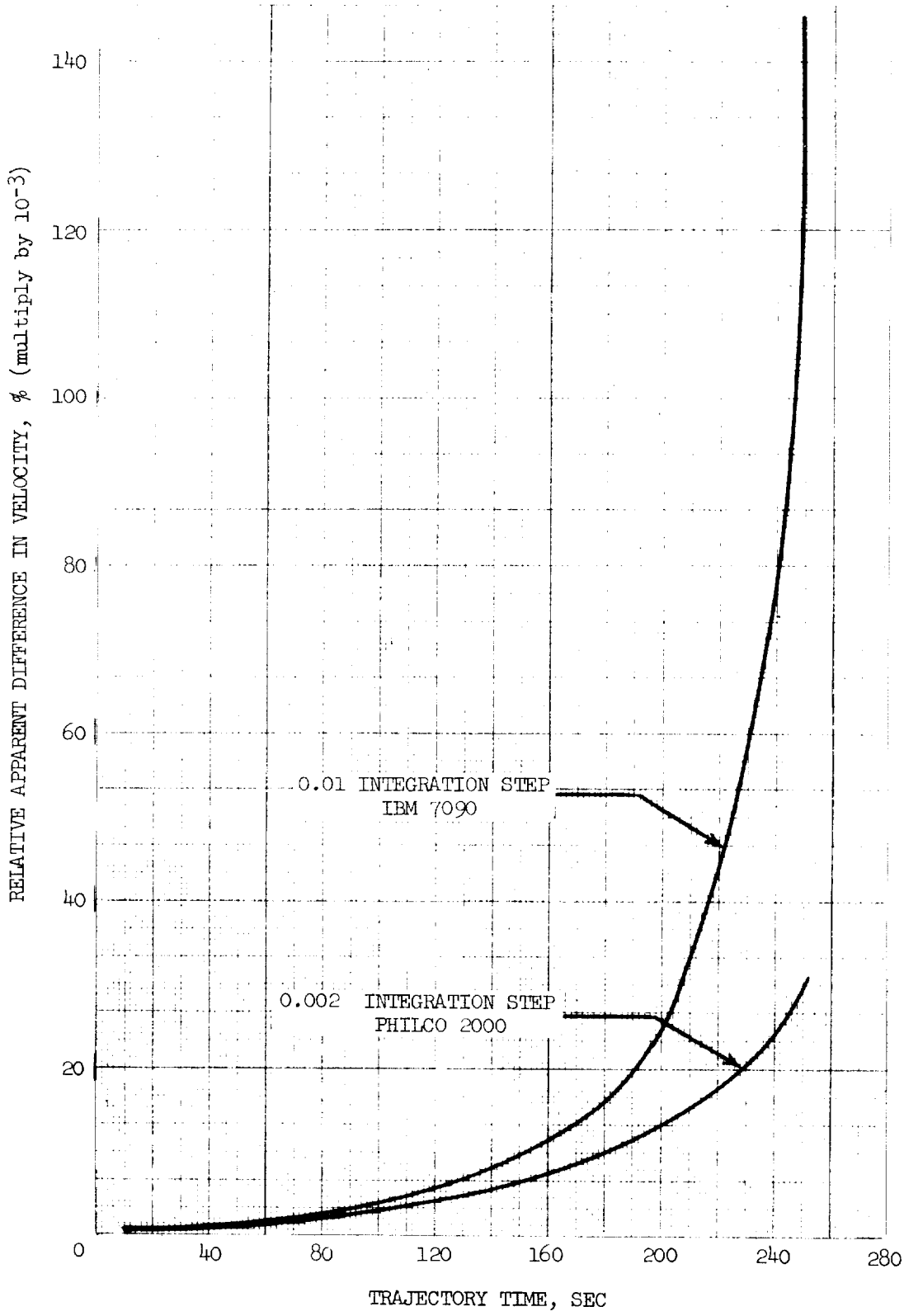

Fig. 11 Influence of Integration Interval Upon Apparent Velocity Error

the classical equations of motion have not been considered, since they are not known by the research staff. However, the terminal point of that solution could be at a trajectory time from 282 to 283 seconds, the apparent termination point of the trajectory.

Two sets of solution data have been reduced to graphical form. The first set consists of those trajectory variables which are provided by either the classical or hodograph equation problem statement, as follows:

1. ν, r vs t (Figure 12)
2. V, γ, V_n, θ vs t (Figure 13)
3. $\dot{V}$ vs V (Figure 14)
4. $\dot{\nu}$ vs ν (Figure 15)
5. θ vs ν (Figure 16).

For general information, these characteristics are presented here without comment. In Figure 13, note that the ordinate scale for the radial velocity (Vr) is five percent (1/20) of the normal and total velocity scale. The second set of solution data consists of the trajectory hodograph variables which are provided uniquely by the hodograph equation problem statement, as follows:

1. $\dot{C}$ vs C and $\dot{R}$ vs R , for 0-250 sec (Figure 17)
2. $\dot{C}$ vs C and $\dot{R}$ vs R , for 250-280.45 sec (Figure 18)
3. $\dot{\phi}$, $\dot{\Psi}$ vs ϕ (Figure 19)
4. $\dot{C}$ vs $\dot{R}$ for 0-14 sec (Figure 20)
5. $\dot{C}$ vs $\dot{R}$ for 14-253 sec (Figure 21)
6. $\dot{C}$ vs $\dot{R}$ for 253-280.45 sec (Figure 22)
7. R vs C (Figure 23)

These characteristics are only a few of those possible for study. Nevertheless, some very interesting and new statements about the trajectory properties can be made, based upon these characteristics. In general, note that the hodograph solution provides direct definition of the instantaneous orbit at each point of the space trajectory. Consequently, upon any contemplated or inadvertent shutdown of the propulsion system enroute, the resulting orbital trajectory of the space vehicle would be directly available for emergency decision or alternative thrust programming.

The characteristics of $\dot{C}$ vs C and $\dot{R}$ vs R (Fig. 17 and 18) were provided for possible study of the energy state changes, comparable to use of the phase plane in the analysis of nonlinear oscillations (Ref. 23). For example, $\dot{C}$ and $\dot{R}$ are specific accelerations rather than potential energy terms, while C and R are specific velocities which are indeed kinetic energy terms. Consequently, the energy state changes may possibly be fruitfully studied in analytic form by use of these characteristics.[1]

[1] Note that the hodograph transformation is intimately related to the Hamiltonian function and its coordinates.

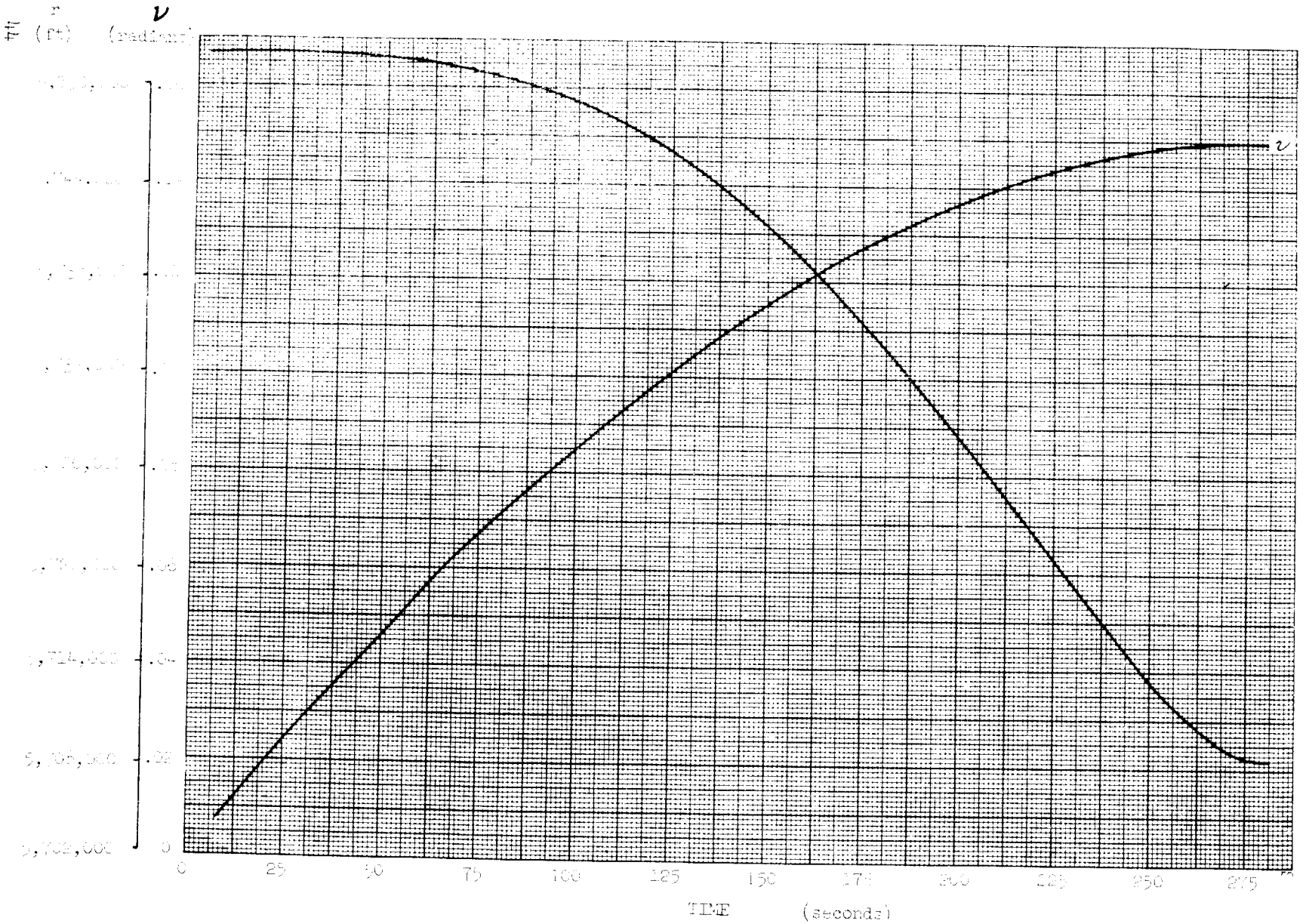

Fig. 12 ν, r vs. t

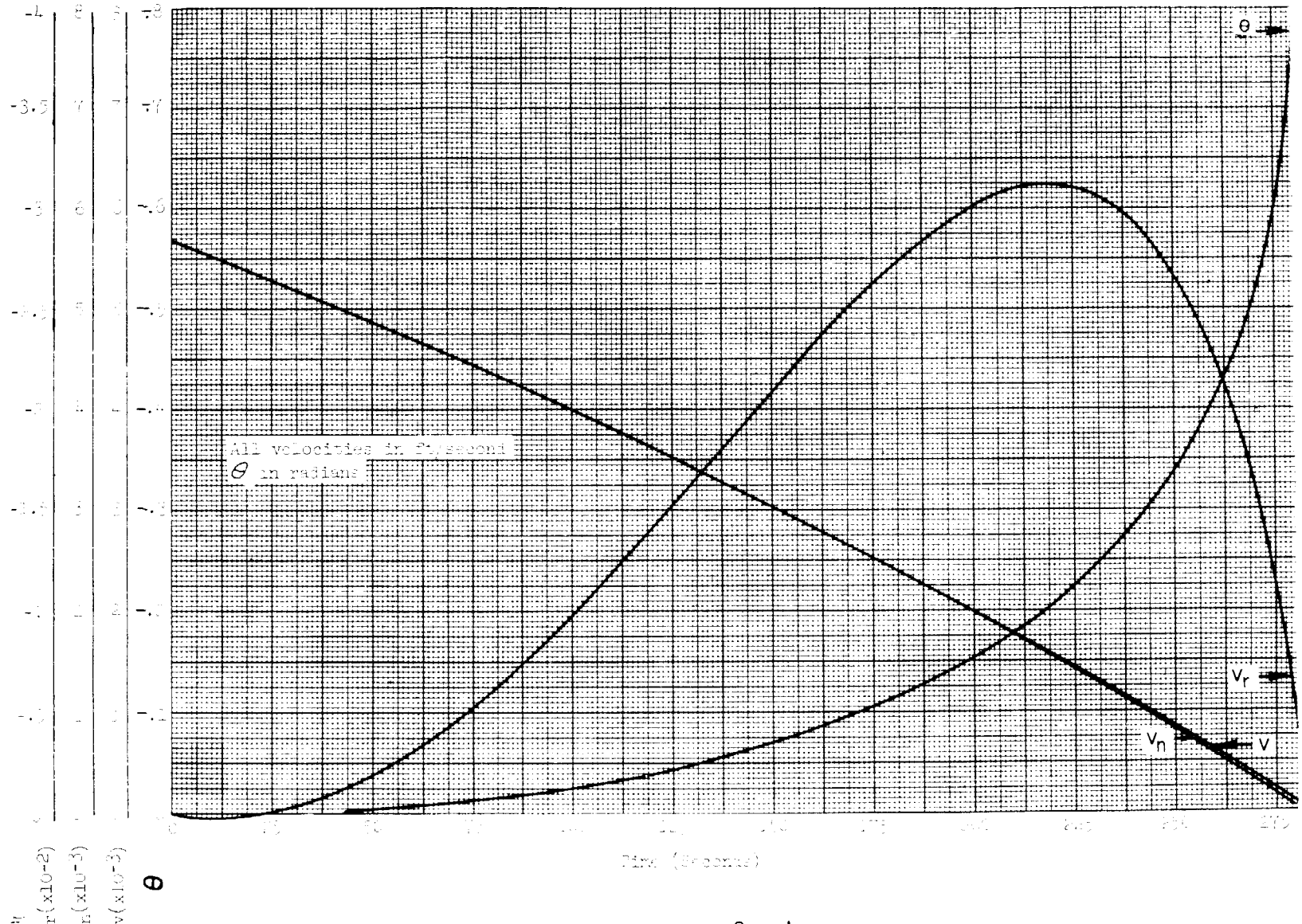

Fig. 13 v, v_r, v_n, θ vs. t

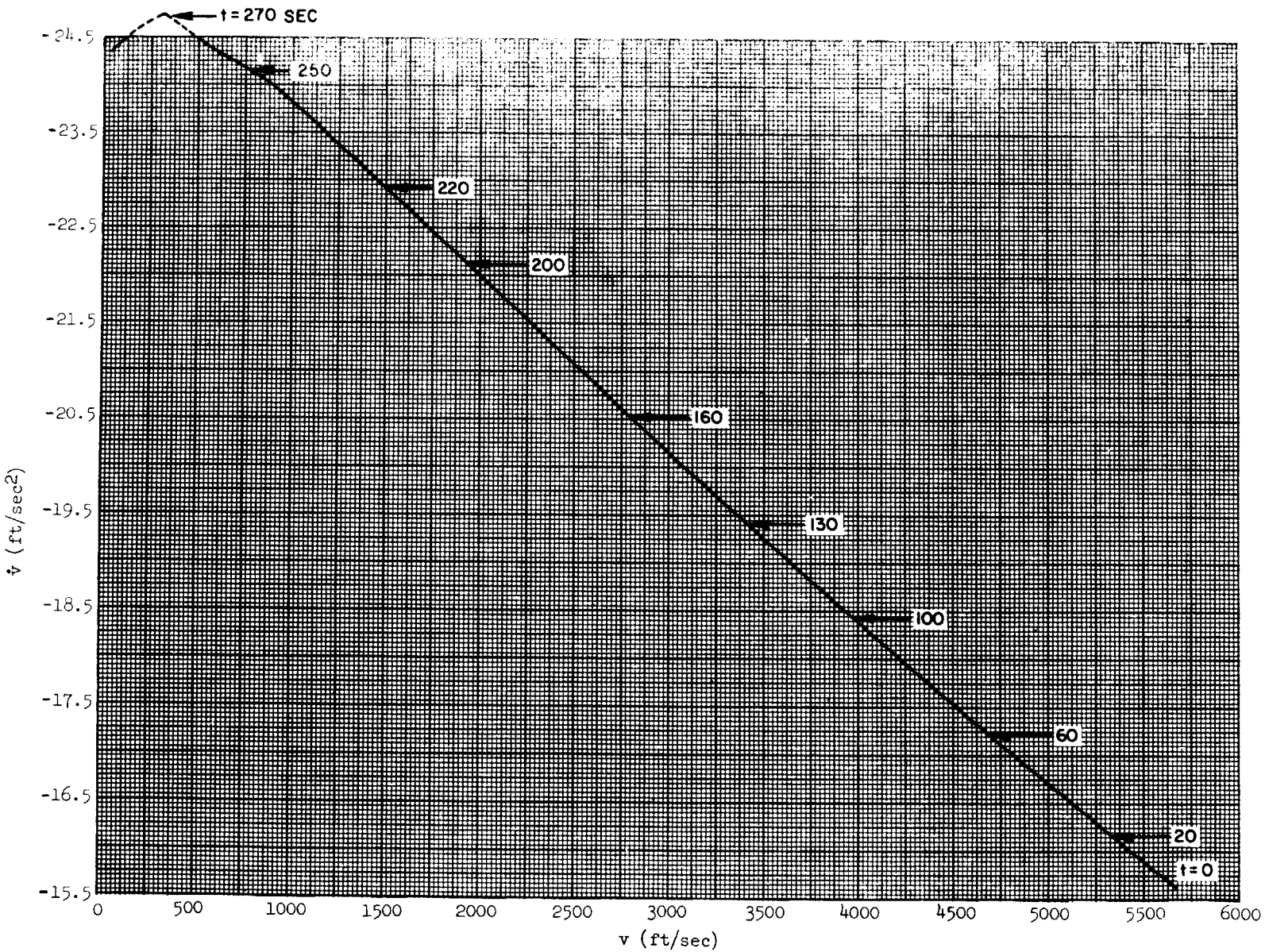

Fig. 14 $\dot{V}$ VS. V

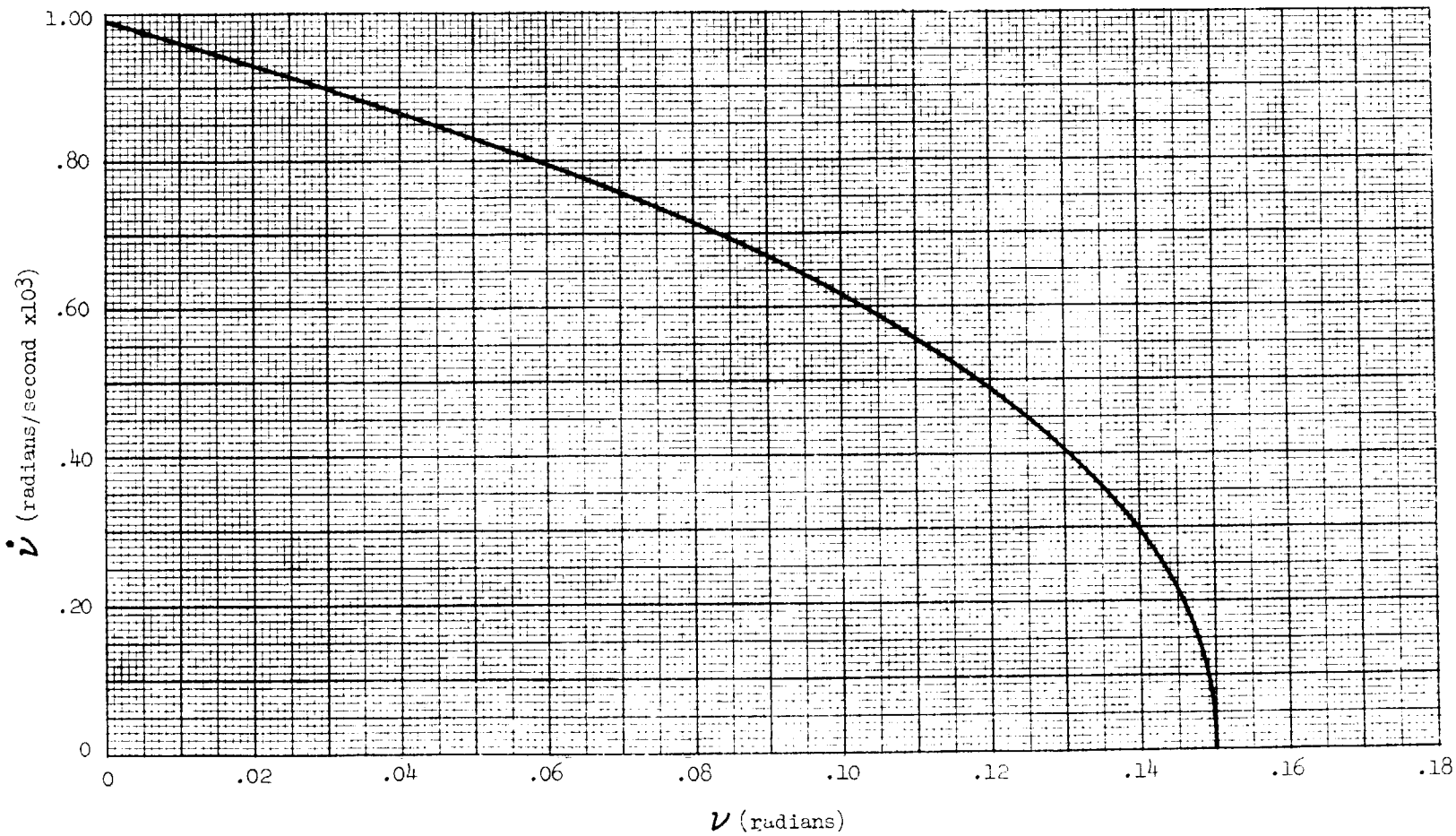

Fig. 15 Graph of $\dot{\nu}$ vs ν

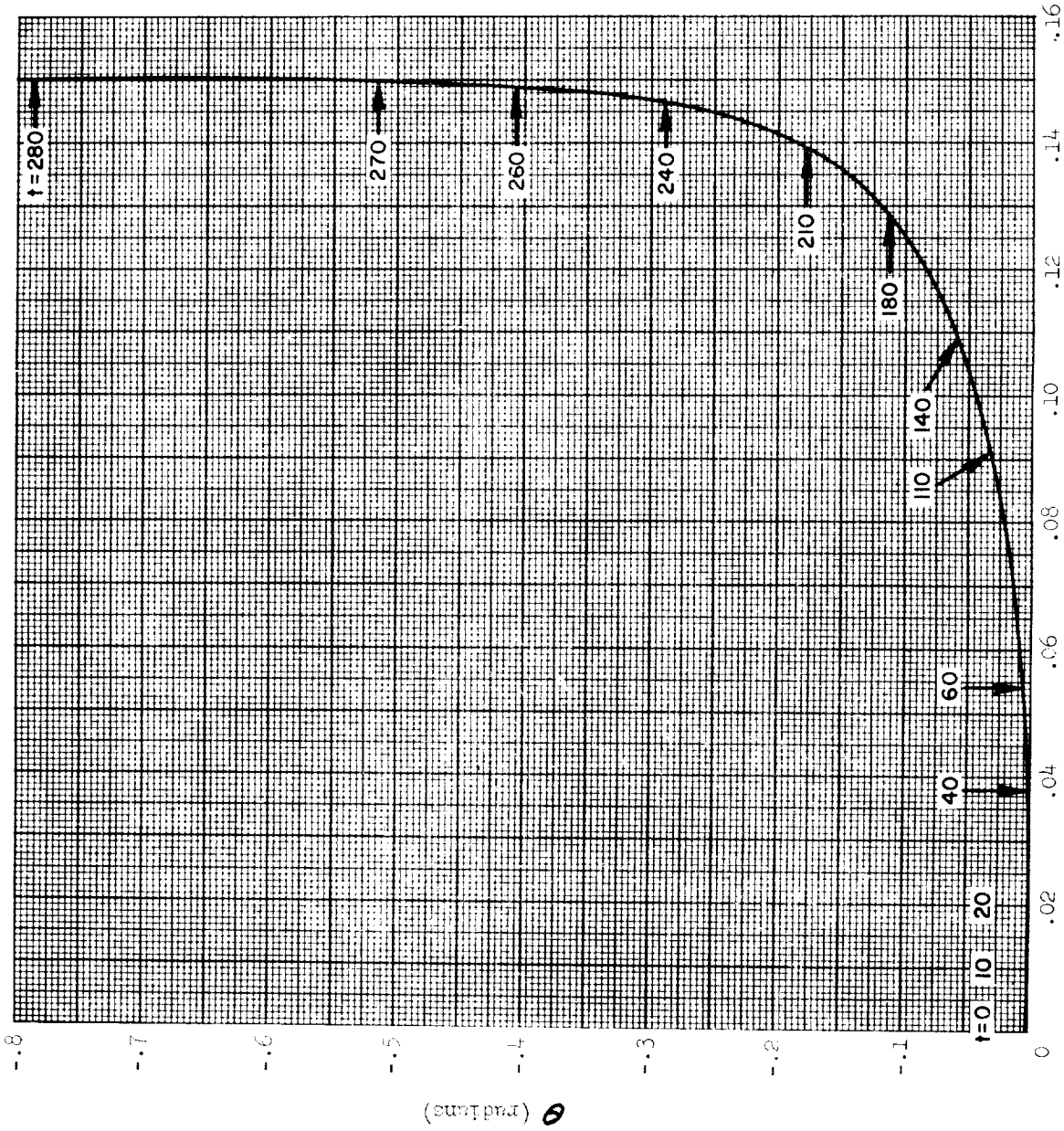

Fig. 16 Graph of θ vs ν

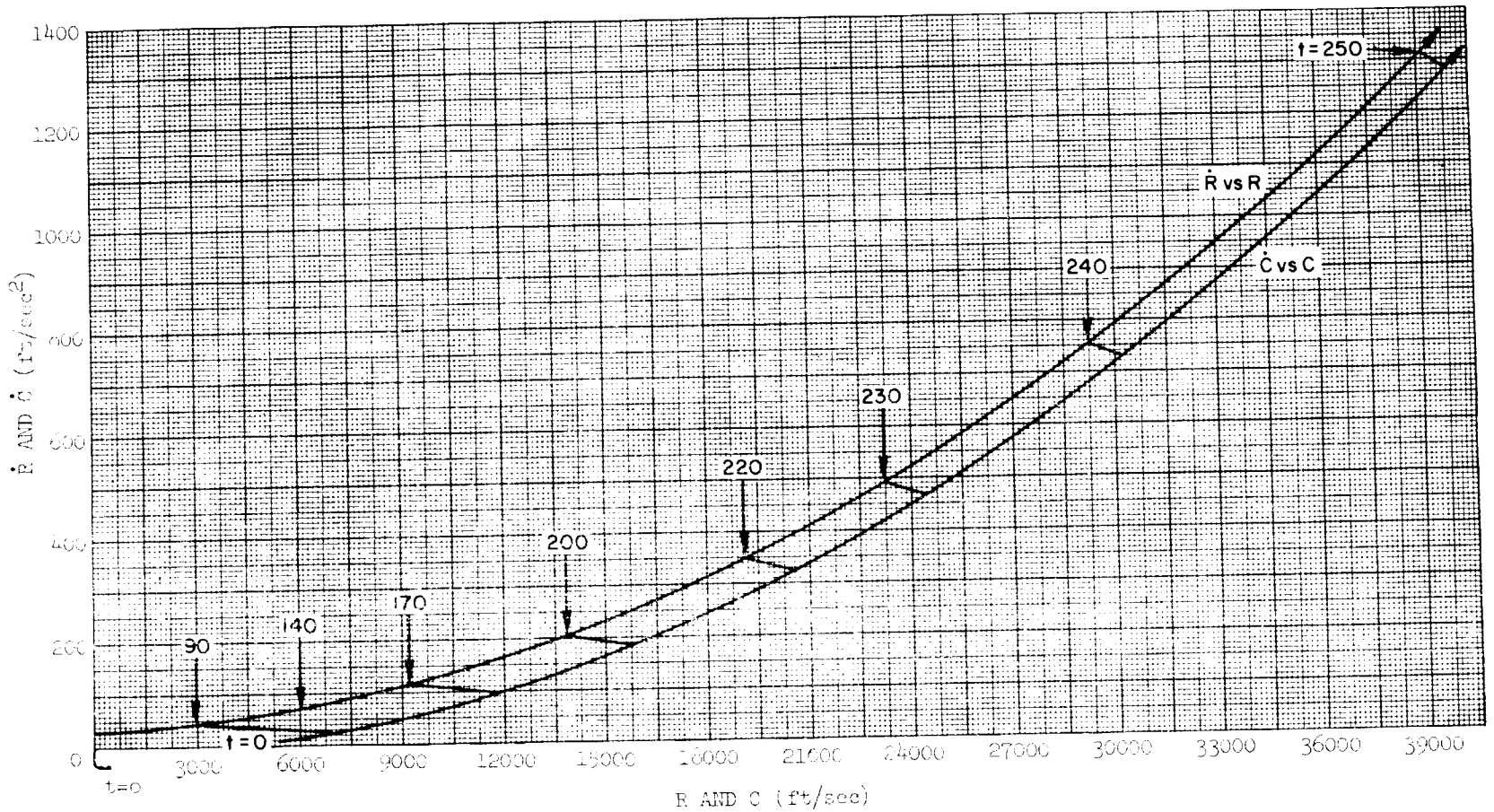

Fig. 17 $\dot{C}$ vs. C and $\dot{R}$ vs. R (0-250 sec.)

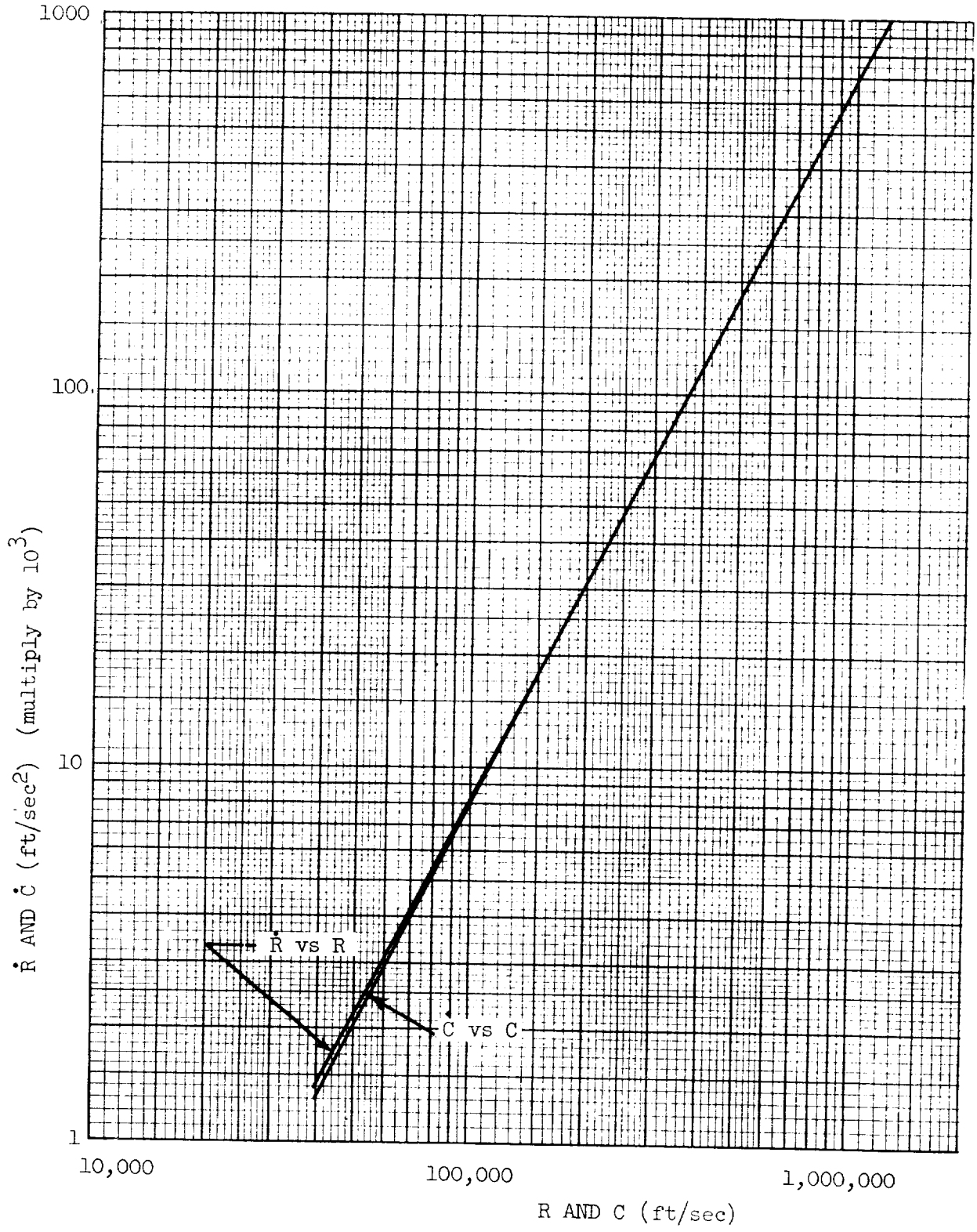

Fig. 18 $\dot{C}$ vs C and $\dot{R}$ vs R (250-280.45 sec)

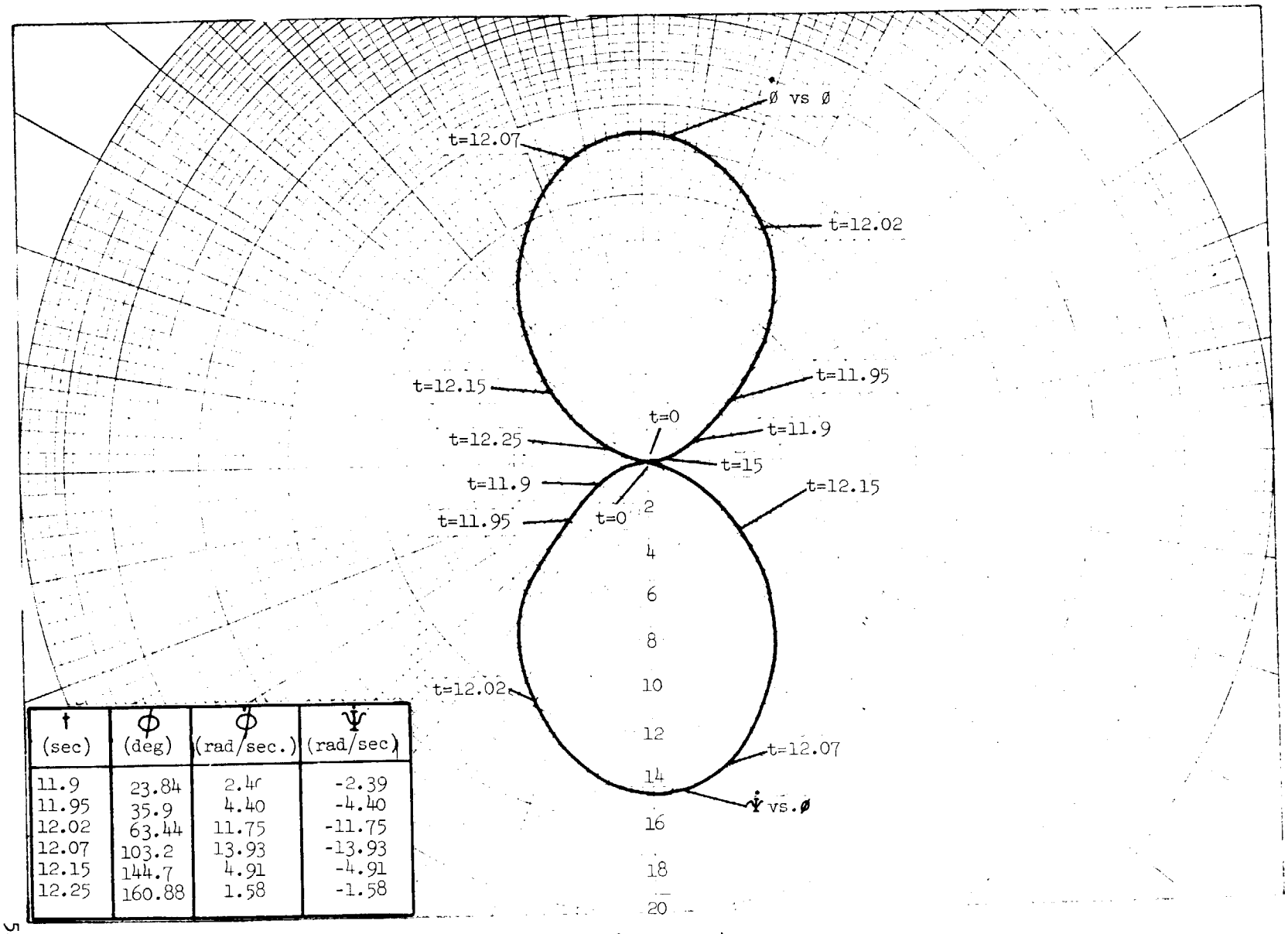

t (sec)	Φ (deg)	Φ̇ (rad/sec.)	Ψ̇ (rad/sec)
11.9	23.84	2.4r	-2.39
11.95	35.9	4.40	-4.40
12.02	63.44	11.75	-11.75
12.07	103.2	13.93	-13.93
12.15	144.7	4.91	-4.91
12.25	160.88	1.58	-1.58

Fig. 19 ϕ, $\dot{\Psi}$ vs. ϕ

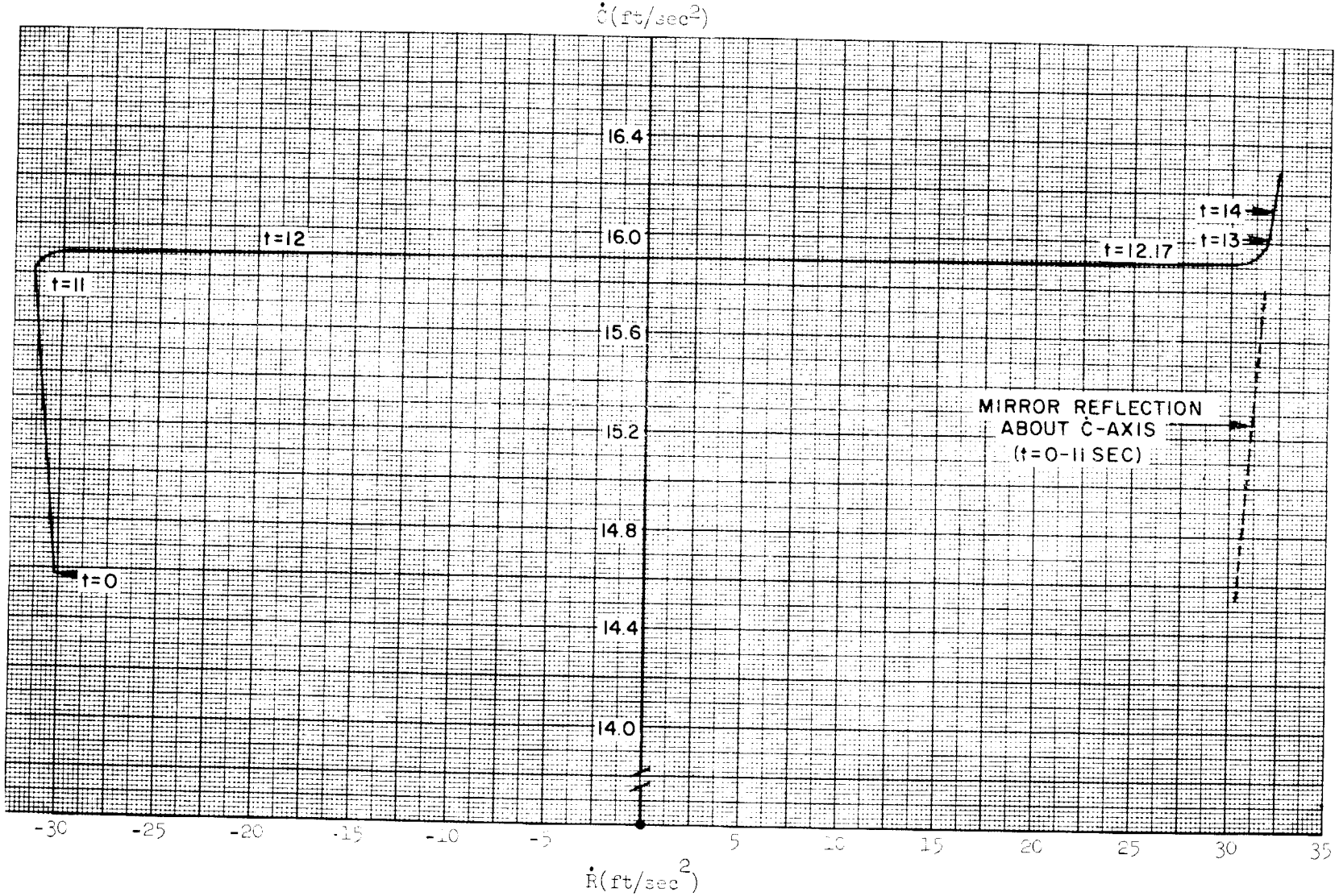

Fig. 20 $\dot{C}$ vs. $\dot{R}$ (0-14 sec.)

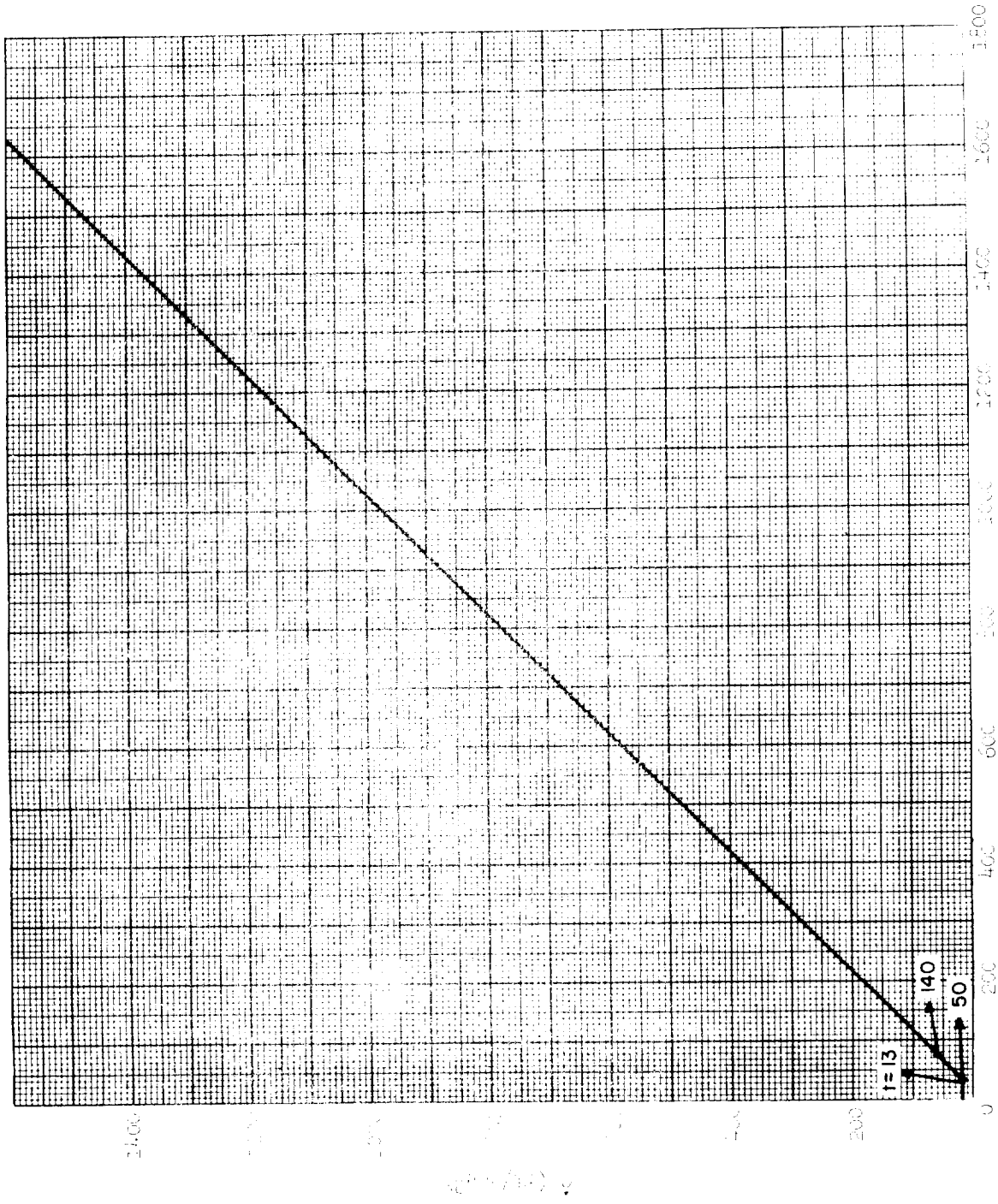

Fig. 21 $\dot{C}$ vs. $\dot{R}$ (14-253 sec.)

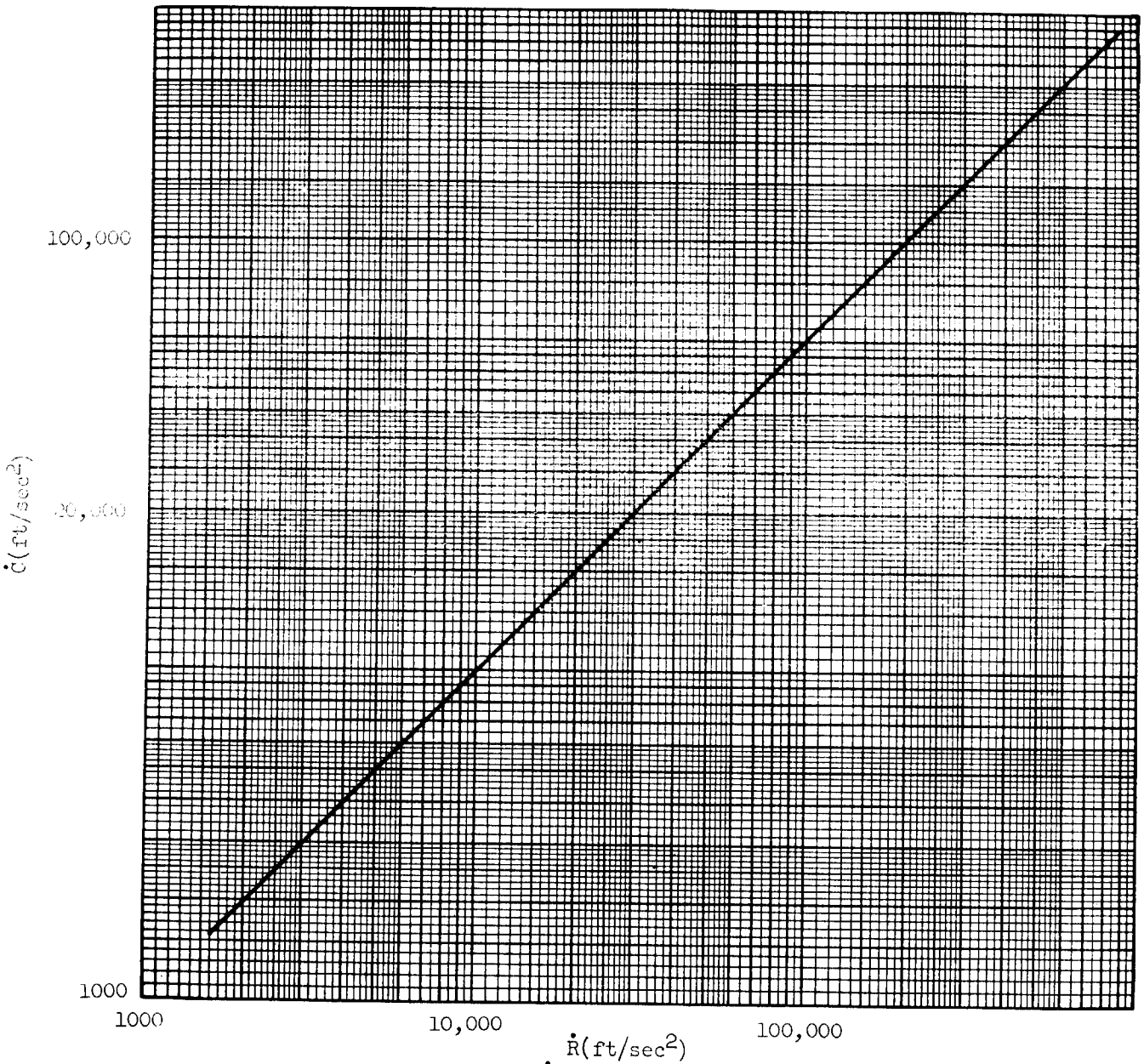

Fig. 22 $\dot{C}$ vs $\dot{R}$ (253-280.45 sec)

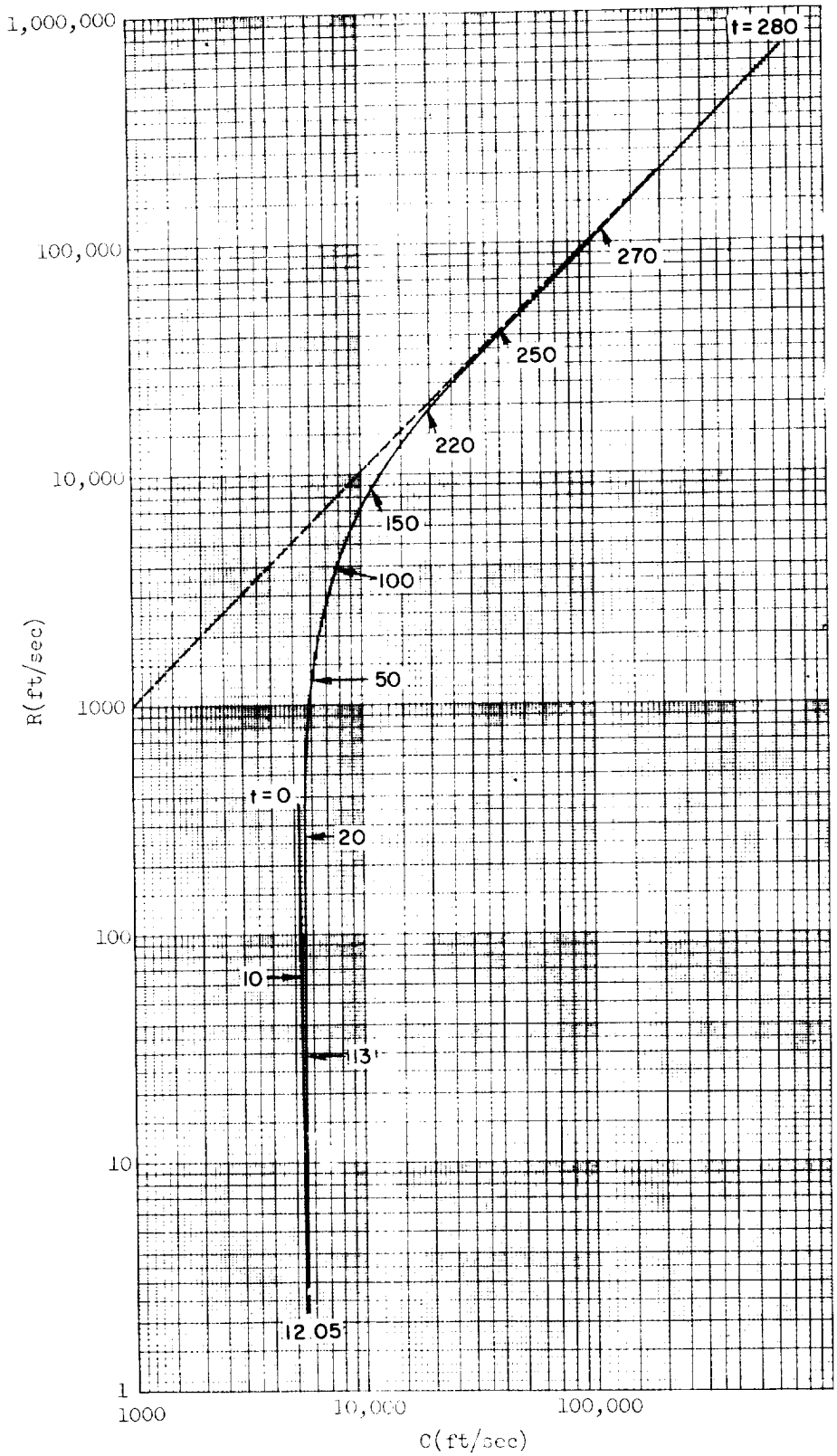
1,000,000
100,000
10,000
1000
100
10
1
R(ft/sec)
1000
10,000
100,000
C(ft/sec)
t = 280
270
250
220
150
100
50
t = 0
20
10
13
12 05

Fig. 23 R vs. C

At this point, consider the variation of the true anomaly rate ($\dot{\phi}$) and the apsidal line rate ($\dot{\Psi}$) with ϕ, as shown in the polar diagram of Figure 19. As seen upon reference to the tabular excerpt of values on Figure 19 for 11.9-12.25 seconds, both $\dot{\phi}$ and $\dot{\Psi}$ (of opposite signs) pass through very large values (e.g., 13.93 radians/second at 12.07 seconds). In essence, the instantaneous hodographs appear to be "rotating" (or flipping over) about 180 degrees. That is, within a very small time interval at about 11-13 seconds, the space vehicle has changed phase position in its instantaneous orbit from the proximity of perigee to the close proximity of apogee. As will become apparent later, the resulting change in vector geometry has a profound effect upon the mathematical description of the trajectory dynamics.

The characteristic of $\dot{C}$ vs $\dot{R}$ is the most immediately interesting of the new data provided by the hodograph equations. Examination of Figures 20-22 shows that two time regimes provide apparently different characteristic behavior: the initial trajectory period from 0 to 14 seconds (Fig. 19), and the "midcourse/terminal" period from 14 seconds on (Fig. 21 and 22). In the initial period, $\dot{R}$ changes from negative to positive value in a very small time interval. The characteristic curve bears a striking resemblance to a switching function, such as encountered in electronic systems and components. Note that the characteristic curve from 0 to 11 seconds provides a mirror reflection (about the $\dot{C}$ -axis of symmetry) which comprises an extension of the linear characteristic from 13 seconds on. Note also that this characteristic for the "midcourse/terminal" phase is remarkably linear, with the slope of the characteristic equal to unity. This initial characteristic leads obviously to speculation on its nature.

It appears that, as the space vehicle departs from perigee of the initial orbit, the positive radial velocity must be overcome by the negative radial acceleration due to thrust (as indicated by negative $\dot{R}$ principally). However, it is not readily apparent precisely why the abrupt transition in sign of $\dot{R}$ occurs, although it is undoubtedly directly related to the basic vector direction change (relative to the local horizon) of the velocity (and consequently the thrust vector). Thus it is seen that this "switching" interval is just that time interval for change in the true anomaly of the instantaneous hodograph, described previously in the discussion on Figure 19.

On the basis of these observations, the following postulate is suggested: If thrust inception occurred at apogee rather than perigee, the "switching" phenomena would not be observed. If this postulate were confirmed (e.g., by machine solution), then the following further observations would become even more significant to analysis and use of the specified thrust program.

At this point, attention is called to the variation of the flight path angle (θ) with time (Fig. 13) and with the space angle (Fig. 16). In the selection of the T and $\dot{m}$ values (see Appendix A), suitable terminal conditions for the final landing on the lunar surface were undoubtedly desired. If final landing were essentially along a lunar vertical, then achievement of a flight path angle (θ) $\approx \pi/2$ is desired as soon as feasible, to enable proper vehicle attitutde orientation. It is suggested that an earlier

attainment of this flight path angle might be provided by inception of this thrust program at other than the perigee passage point. In the present parameter selection, the path angle changes from about 45 degrees at 280 seconds, to 90 degrees at about 283 seconds.

The $\dot{C}$ vs $\dot{R}$ characteristic for the "midcourse/terminal" phase is remarkably linear to the limit of machine solution accuracy, as noted above. Consequently, this characteristic may be formulated very accurately, in this trajectory phase, by the following equation:

$$\dot{C} = \dot{R} + K \tag{119}$$

where $K \approx -25$ fps^2. From this, we obtain

$$C = R + K(t - t_i) + (C_i - R_i) \tag{120}$$

where C_i and R_i are corresponding given values at the initial time reference t_i (e.g., t_i may be selected as 14 seconds on the trajectory program). These additional relations may enable further insight into analytic solution of the original, complete lunar landing hodograph equations (see Table III), or be used directly for analytic solution form valid for most of the trajectory. Due to the lack or further study time, such investigation has not been attempted.

Finally, the characteristic of R vs C is presented in Figure 23. The significance of this characteristic stems from the orbital energy diagram (Ref. 4) represented by R^2 vs C^2, as shown in Figure 24. The R vs C characteristic is presented, rather than R^2 vs C^2, for concise presentation with a reduced scale range. It is seen that in the initial trajectory phase (up to $t \approx 12$ seconds), the instantaneous orbital energy decreases; in the "midcourse/terminal" phase ($t > 12$ seconds), the instantaneous orbital energy increases, approaching zero energy represented by the zero eccentricity line (shown dotted in Fig. 23) for the terminal point. In order to be consistent with the previously suggested postulate, this characteristic would not show decreasing energy for thrust inception from apogee. Note that this characteristic provides direct qualitative evaluation of the instantaneous orbital energy along the trajectory, with only a scale change required for direct quantitative evaluation.

The computer program for the hodograph equations of motion, together with trajectory run data, is available at Corporate Systems Center for future reference and use as desired.

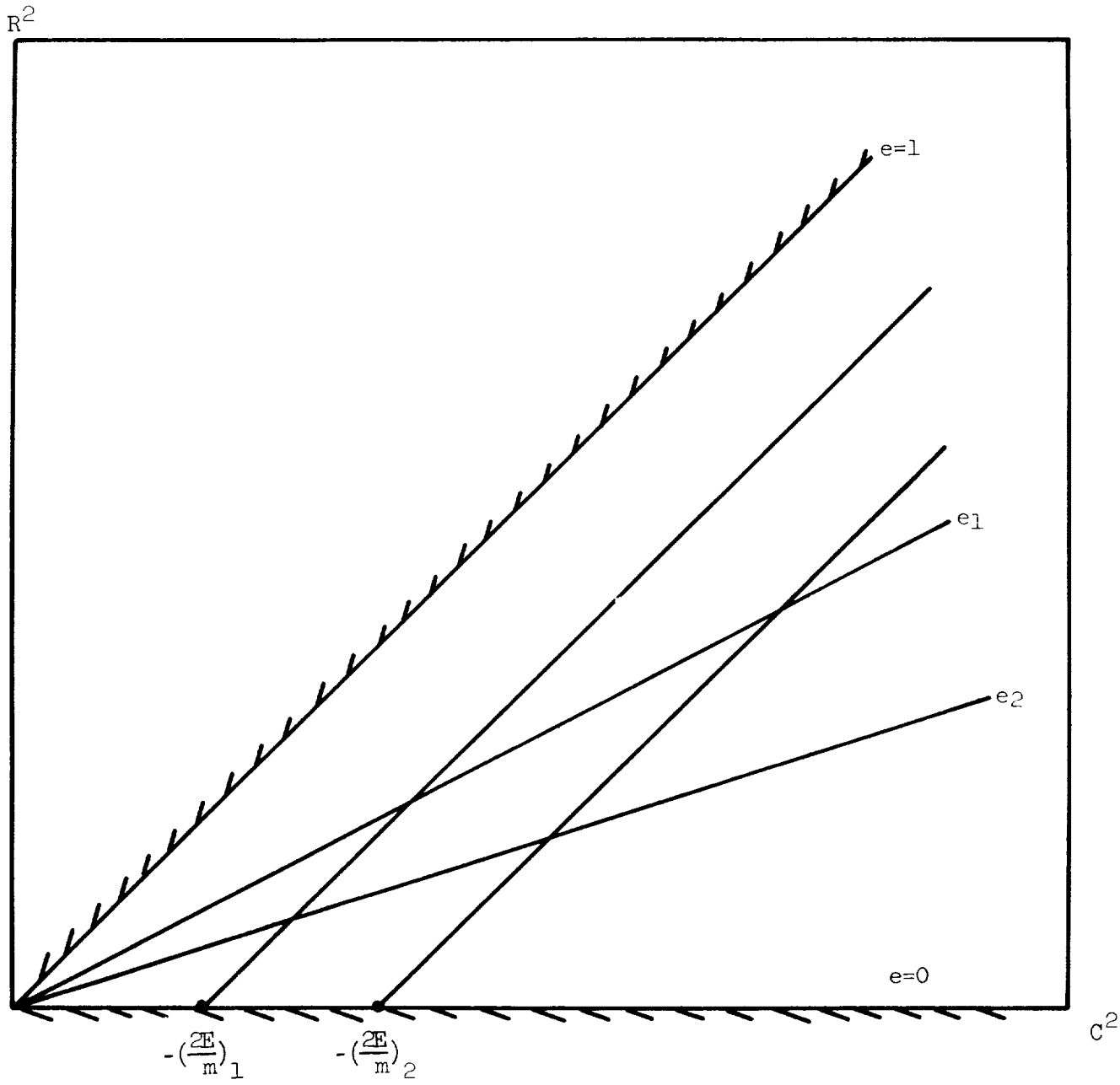

Fig. 24 Orbital Energy Diagram

VIII. TRANSFORMATION THEORY AND CHARACTERISTICS

The basic equations of the acceleration hodograph transformation have been determined, and one problem application has been studied. However, the scope of the transformation theory required for complete application and use is far greater than covered by this initial study effort.

First, let us consider the general statements possible about the transformation theory established as of this time. The equations of motion, when transformed by use of the hodograph variables, are principally comprised of trigonometric (i.e., transcendental) functions (see Eq. 52B, 53B, 56A). However, the functional forms of the equations are quite simple in structure, and of low differential order and of first degree. Consequently, both analytic treatment or manipulation and machine computation are significantly facilitated.

For example, it was found that the computer programmers found the transformed (i.e., hodograph) equations much simpler to program and check out, largely due to the need for only one integration compared with two integrations required for the original (i.e., nontransformed) equations. The ease of applying diagnostic procedures to test the program can become extremely important in large scale programs for use in large space system mission and trajectory computation and simulation.

Second, the transformed equations of motion are regularized with respect to all classes of real orbit. That is, no singularities are encountered within the real regions of solution, such as are encountered with a conic parameter formulation of the orbital trajectory or perturbation therefrom. Consequently, the variation-of-parameters method of describing the trajectory class and its perturbation equations can be effectively used without restriction or special conditions required. While this statement is also applicable to Herrick's "universal variables" and resultant equations, this hodograph transformation results most directly and naturally from the original equations, without mathematical manipulation to obtain mapping functions. That is, the hodograph parameters have direct physical significance, enabling the direct mapping of all trajectory characteristics over into the space or velocity planes.

Third, the hodograph variables and the transformed equations of motion can be directly presented graphically, due to their geometric properties. This characteristic property has been effectively demonstrated by the geometric presentation of the instantaneous velocity and acceleration hodograph terms of the lunar landing problem (see Fig. 9). This geometric presentation should be generally possible, since it is also true for the impulsive thrust analysis (Ref. 2). This graphical interpretation appears of outstanding importance, second only to the possible ease of analytic treatment of powered trajectories. The need for readout and display of the significant characteristics of a trajectory has become most critical, in this era of extremely complex systems and attendant computation requirements. For a completely automatic system,

an appropriate display is essential for monitoring and diagnostic test procedures for large-scale or high-speed machine computation. For an integrated man-machine system, an effective display of trajectory characteristics appropriate for the optimum use of the human operator's decision capability is mandatory. The hodograph transformation provides problem statement, treatment, and solution with analytic rigor, while simultaneously enabling the real-time display of all essential performance characteristics provided in the most effective relationships, as required.

Fourth, it is apparent that the specified mass variation function (or "law") has a profound effect upon the possible analytic procedures and application utility. The problem application considered in this initial study program specified that the vehicle mass be a function of time. Consequently, analysis of the hodograph equations of motion required the integration procedure for complete solution, rather than the differential geometry approach. As mentioned previously, the differential geometry analysis requires the elimination of time explicitly as the independent variable. Since this condition could not be met with the stated lunar landing problem, only analytic integration was attempted. For this reason, the differential geometry techniques were not studied in greater detail. If the mass variation were a function of space, velocity, or acceleration coordinates, then the use of the differential geometry approach would be available.

This one point, i.e., elimination of time from the hodograph equations, is so basic to the potential use of the hodograph transformation, that its feasibility is discussed in greater detail here. The velocity hodograph transformation has been quite powerful in providing new solutions for the impulsive thrust program, because time is not present in the problem equations. (However, it should be noted that time relations can be provided as auxiliary equations, as desired.) As shown in previous sections on the basic derivation of the hodograph equations, time in explicit form is absent from the basic equations of motion in every term except the mass variation. At this point, it is reasonable to ask whether the mass variation, as provided in the equations of motion, can ever be other than dependent upon time explicitly.

Considering the propulsion control only, i.e., as an open-loop or regulator function solely, the mass-variation is obviously a time-dependent function. However, if this fuel flow control or basic servo element is used in a closed-loop mode of operation, the mass-variation will become a function of the error-sensed variable, since the time-dependency is then only due to servomechanism lags. If the closed-loop operation is satisfactory, such lags will be negligible in effect. It should be clear that the fuel flow control will always be used as a servo element in closed-loop operation. Consequently, the following general statement on space system synthesis and design is proposed: <u>The inner closed-loop (or loops) of which the fuel flow control is a servo element may be designed so that mass-variation is a function of space, velocity, or acceleration coordinates rather than time</u>. Then the hodograph equations of motion for the space vehicle would be independent of time as an explicit variable, enabling the use of differential geometry

solution for trajectory classes rather than analytic integration for solution.

This suggested trajectory synthesis and analysis procedure is a sharp break with traditional trajectory study practice currently in common use. Although closed-loop system theory has become a dominant factor in space system technology for hardware design, its influence upon mission analysis and trajectory design has been quite limited and only recently recognized. The principal influence has been the application of filter theory (e.g., Ref. 24) and dynamic programming (e.g., Ref. 25) to these problems. Much of this work has been carried out by Ames Research Center (NASA) and the Rand Corporation. The proposed change in the treatment of the vehicle mass-variation is deterministic, enabling the use of all prior trajectory synthesis and analysis techniques but with widely extended possibilities for analytic solution. The research staff on the present study considers this proposal as feasible and realizable from the viewpoint of mechanization technology, as well as desirable and promising from the viewpoint of extension and completion of trajectory solutions, and understanding of the properties of classes of powered trajectories.

Aside from the aforementioned application of filter theory and dynamic programming, the direct use of optimization programs (e.g., by use of the variational calculus) to study trajectory classes, comprises a break with traditional trajectory synthesis and analysis practice. Such trajectory study is at least as restrictive or limiting on design practice as the proposed treatment of the mass-variation.

Before proceeding to the final section of this research study report, some brief comments upon the lunar landing problem are timely. The desired analytic (or closed-form) solution was not obtained by the research staff. However, the transformed equations of motion are so relatively simple in form that future solution might be attained by their use, upon subsequent study by more skillful mathematicians or analysts.

It should be noted that the specified terminal condition for zero velocity at a finite distance from the attracting center of the celestial body defines a singular point in the field of solution for the hodograph transformation. That is, this condition defines a point on an orbit which passes, in the theoretical sense, through the attracting center of the celestial body. Such orbits comprise singular solutions in the hodograph transformation and equations. Consequently, machine computation accuracy degenerates within the neighborhood of this terminal point; i.e., the endpoint hodograph solution is indeterminate. The hodograph transformation regularizes all orbits with singular points at infinite distances from the attracting center. However, it is interesting to note that the valid region of machine solution for the hodograph equations extends quite close to the singular endpoint (see Section VII-D). This computational validity is especially interesting for possible re-entry studies by use of hodograph equations, as proposed in Section IX. Since computational accuracy can be attained with the hodograph equations for relatively small magnitudes of velocity vector, such re-entry study is feasible.

IX. RECOMMENDED AREAS OF FUTURE RESEARCH STUDY

It has been noted that this research study comprises an initial investigation of the acceleration hodograph transformation. The basic general equations have been defined, the orbital (i.e., ballistic) acceleration hodograph studied, and one problem application for an arbitrarily specified thrust function has provided hodograph equations of motion for a vehicle subject to that thrust function.

The transformation theory is clearly far more extensive than studied to date, while application techniques have not been treated comprehensively due to broad scope. Also, in the course of study, many promising areas for future study have become apparent, and are presented here for consideration. Assuming that the initial study results and the proposed study areas appear promising for potential advancement of two-body space trajectory synthesis and analysis techniques, the formulation of subsequent study objectives may be aided by these study suggestions.

Future study may be suitably classified as an extension of the application scope, investigation of basic characteristics of the application equations, program mechanization techniques, and the lunar landing problem. The major topics extending the application scope are

1. Formulation of the three-dimensional equations
2. Analytical treatment of oblateness effects
3. Development of the hodograph equations for motion in molecular or sub-molecular media

The major topics for investigation of basic characteristics of the application equations are

1. Development of realizable and useful mass-variation functions
2. Development of hodograph generation techniques by use of the differential geometry
3. Energy relations
4. Time relations
5. Evaluation techniques for impulsive vs continuous thrust functions

Program mechanization includes

1. Computation
2. Optimization
3. Situation displays
4. Abort emergency command and control

A. Extension of the Application Scope

This initial study has formulated the hodograph equations of motion in two-dimensional space. Obviously, its extension to motion in three-dimensional space will enable treatment of complete space trajectory problems. Just as the two-dimensional formulation of the velocity transformation equations (Ref. 2, 8) has been effectively and simply extended to three-dimensional space (Ref. 9), the three-dimensional formulation of the acceleration transformation equations is seen as a clear and direct analytical procedure. As noted in Section V, the three-dimensional vector notation (Ref. 18) is a most effective formulation method. For example, it can be shown that

$$\bar{v}=\bar{C}\times\left[\frac{\bar{R}\times\bar{C}}{C^2}+\bar{i}\right] \tag{121}$$

where $\bar{R}$ and $\bar{C}$ are hodograph vectors directed as defined in the Nomenclature. As part of this study extension, it is suggested that the contents of Reference 26 might be reviewed and correlated with the formulation results.

The hodograph equations are valid for the potential field of a regular, spherical celestial body. That is, the higher order terms of a spherical harmonic expansion for the gravitational potential field have been neglected. The triaxiality terms which more accurately describe the real physical problem will affect the solutions, especially for the synthesis and analysis of long-term trajectories (e.g., of time duration greater than one nominal orbital period). For most trajectory problems other than the long-term orbit maintenance required for communication satellites, the oblateness effects are generally sufficient for synthesis and analysis consideration. That is, consideration of the spherical harmonics due to the first order difference from the regular sphere (or oblate spheroid) are generally adequate for the additional accuracy which may be required for long-term trajectories. Then the J-term of the harmonic expansion

$$V=-\frac{\mu m}{r}\left[\frac{r_e}{r}+J\left(\frac{r_e}{r}\right)^3\left(\frac{1}{3}-\cos^2\eta\right)+\cdots\right] \tag{122}$$

accounts for the oblateness effects upon the line of apsides (Ψ) and the line of nodes (Ω). As shown by Blitzer, Weisfeld, and Wheelon (Ref. 27-29), the apsidal and nodal line rotations due to oblateness, in each orbital period (or revolution) are closely approximated by

$$\Delta\Psi_J=2\pi J\left[\frac{r_e}{a'\left(1-e^2\right)}\right]^2\left(2-\frac{5}{2}\sin^2 i\right) \tag{123}$$

$$\Delta\Omega_J=2\pi J\left[\frac{r_e}{a'\left(1-e^2\right)}\right]^2\cos i \tag{124}$$

By use of Equations 123 and 124, and using a time average for the apsidal and nodal line rotations

$$\dot{\Psi}_J \approx \frac{\Delta\Psi_J}{2\pi/n} = Jn\left[\frac{r_e}{a'(1-e^2)}\right]^2 \left(2-\frac{5}{2}\sin^2 i\right) \tag{125A}$$

$$\dot{\Omega}_J \approx \frac{\Delta\Omega_J}{2\pi/n} = Jn\left[\frac{r_e}{a'(1-e^2)}\right]^2 \cos i\ . \tag{126A}$$

However,

$$n = \frac{(C^2-R^2)^{\frac{3}{2}}}{\mu} \tag{48}$$

and

$$a'(1-e^2) = \frac{\mu}{C^2} \tag{49}$$

so that

$$\dot{\Psi}_J = J\left(\frac{C}{v_{ce}}\right)^4 \frac{(C^2-R^2)^{\frac{3}{2}}}{\mu} \left(2-\frac{5}{2}\sin^2 i\right) \tag{125B}$$

$$\dot{\Omega}_J = J\left(\frac{C}{v_{ce}}\right)^4 \frac{(C^2-R^2)^{\frac{3}{2}}}{\mu} \cos i\ . \tag{126B}$$

Consequently, either the hodograph transformation or the equations of motion themselves may be modified to account for the oblateness effects, if required. First, in the original formulation of the hodograph parameters (see Section V), the J-term of the potential function may be included in the energy equation. Hence, modified hodograph parameters may be developed. As an alternative, the major apparent effects upon the instantaneous orbital parameters, as described by Equations 125B and 126B, may be treated as perturbations. That is, in the vector equation

$$\ddot{\bar{r}} = \left(\Delta a_r - C\dot{\nu}\right)\bar{T} + \left(\Delta a_n\right)\bar{J}\ , \tag{56B}$$

the apsidal and nodal line rotations due to oblateness effects would be seen as part of the applied accelerations (Δa_r, Δa_n). Either approach appears feasible and tractable for synthesis and analysis. However, at this time, the latter approach appears more amenable to mathematical treatment.

Aside from the simplifed form of the assumed potential field, the basic energy equation and the resultant equations of motion are valid only for motion in a vacuum, or nonresistive medium. However, other media may be

encountered which could cause drag forces upon a space vehicle. The gaseous atmosphere of a planet obviously constitutes such a medium. Also, clouds of microparticles may be encountered in interplanetary space. In both cases, the medium is principally composed of molecular matter. It is interesting to note that Jacobi (Ref. 30) speculated upon and briefly treated this possibility. However, ionic or submolecular clouds may be even more common, or significant to vehicle motion, than microparticle clouds. Consequently, analytical treatment of such forces, which result from passage through a resistive medium, by the hodograph equations could be of great potential use. In this respect, the work of Reference 31 is noted as an early attempt to interpret the atmospheric re-entry problem in terms of the instantaneous hodograph.

In general, the resistive forces are a function of the relative velocity between vehicle and medium. Consequently, treatment of these forces in the original basic equations or as perturbation forces (see Eq. 56B) can be expected to provide promising equations of motion for solution and/or computation. Briefly, consider the following functional relation which approximates the terrestrial atmospheric re-entry forces:

$$f = K_d \sigma v^2 \tag{127}$$

where

$$\sigma \approx \sigma_0 \exp\left(-\alpha r\right) \quad . \tag{128}$$

It is clear that the force varies directly as the product of velocity squared (v^2). and a transcendental function of the normal velocity (v_n) since the exponential term of Equation 128 is related to the normal velocity by Equation 36. Since the difficulties of analysis with the resultant equations cannot be evaluated without further study, such investigation is recommended in view of the potential value for advanced re-entry problems. Note that the functional relation for forces due to interplanetary resistive media will probably not be related to position coordinates, but only to velocity coordinates directly.

B. Investigation of Basic Characteristics of Hodograph Equations

It has previously been noted that mass-variation functions of space, velocity, or acceleration coordinates, rather than of time explicitly, would enable the possible generation of the powered trajectory hodograph directly, without analytic integration of the hodograph equations. It is recommended that realizable and useful mass-variation functions of space, velocity, or acceleration coordinates be postulated and studied. This investigation should be conducted concurrently with the development of hodograph generation techniques.

The generation of a powered trajectory hodograph may be obtained by formal application of the differential geometry. It is suggested that such generation techniques be developed. As part of such study, the oblateness effects due to potential field harmonics as well as drag forces of a resistive medium, might be considered.

The powered trajectory hodograph should enable the derivation of energy relations for the instantaneous thrust energy and orbital energy, as a function of coordinates in the hodograph plane. With such energy relations, the relative merits of various trajectories and thrust programs could be readily evaluated. In addition, the orbital energy diagram (Ref. 4) may prove useful in such study.

For direct utility, any solution generated in the hodograph plane or upon analytic integration should ultimately be expressed in time explicitly. Consequently, as originally proposed, the time relationships should be determined.

It is clear that an infinite choice of thrust programs is available to provide a realizable trajectory between specified sets of endpoint conditions. In general, the relative merits of thrust programs for essentially impulsive (or high level) thrust vs essentially continuous (or low level) thrust are not well understood. While specified optimization of fuel and time constraints permits some statements about specific performance characteristics to be made, relative evaluation criteria are generally unavailable, especially when optimization criteria are not specified. If the previously noted development of hodograph generation techniques, and energy and time relations were substantially successful, then the development of such evaluation criteria would be apparent. Consequently, the development of such criteria is recommended, upon prior satisfactory completion of the above proposed studies.

C. Program Mechanization

The basic nature of the hodograph equations enables the trajectory synthesis and analysis to be treated completely in the hodograph plane, both for powered and ballistic flight, without the need for analytic integration (excepting possible mass-variation functions of time). Consequently, it has been apparent that trajectory computation for machine solution might be simpler and faster with at least equivalent accuracy. The relatively simple computation programming of the lunar landing problem showed that programming was much simpler, and the effective use of diagnostic techniques was considerably easier. Consequently, the use of the hodograph equations for a real space system problem should be considered.

For example, the set of conventional equations used in the Gemini computation program could be transformed into hodograph equations analytically, and subsequently programmed. The two programs could then be studied and evaluated from the viewpoint of programming ease and reliability, computation speed and accuracy, and amenability to diagnostic procedures.

As a result of the extensive use of machine computation for problem solution of space trajectories, the development of machine techniques of optimization (e.g., with the variational calculus or dynamic programming) has become quite attractive. It became apparent, in the velocity hodograph studies, that many optimizations are possible with the hodograph equations, in analytic form. Consequently, it is recommended that optimization criteria and solutions be studied, as applied to the hodograph equations of motion.

In complex computation programs, effective display of the most pertinent characteristics for effective monitoring is becoming increasingly important and critical. The geometric interpretation of hodograph relations, and the algebraic form of the possible transformations between space, velocity, and acceleration coordinates indicate that the hodograph equations are extremely suitable for direct data readout and situation displays. The broad choice of characteristic data available from the transformations provides considerable design freedom for the human engineering and display system designers.

If thrust should unexpectedly be shut down due to failure or emergency conditions, the hodograph equations provide the resultant ballistic trajectory directly, without auxiliary computation or modification. Also, the simpler computation as well as the possibility of analytic solutions indicates that real-time (or shorter) solution for the powered or ballistic trajectory is feasible. Consequently, emergency command and control by a ground control center or an onboard astronaut may be very effectively mechanized by the hodograph equations.

It is suggested that both system design areas of situation displays and emergency command and control be studied for possible application of the hodograph equations and application techniques.

D. Lunar Landing Problem

Further work on possible analytic solution for the lunar landing problem appears quite attractive, especially if this thrust program is of continuing real interest. As noted in the section on machine solution, new approaches which have not been exploited due to lack of research time have become available. In any case, the possible interpretation of the trajectory dynamics from the energy viewpoint appears promising for potential extension of the application techniques. That is, the theory developed for the nonlinear mechanics may lead to further understanding or solutions, upon its application to a given problem such as the lunar landing problem formulated by the hodograph equations of motion.

X. ACKNOWLEDGEMENTS

This research study was conducted by the senior staff, Samuel P. Altman and Josef S. Pistiner, with technical support by Robert A. Lerman, Robert J. Gurka, and Bruce B. Clawson.

XI. REFERENCES

1. Altman, S.P., "Orbital Transfer for Satellites", Proceedings of the Fourth Ballistic Missile and Space Technology Symposium (1959), Pergamon Press 1961, pp. 132-144.

2. Altman, S.P. and Pistiner, J.S., "Hodograph Analysis of the Orbital Transfer Problem for Coplanar Nonaligned Elliptical Orbits", ARS Journal, Vol. 31, No. 9, September 1961, pp. 1217-1225.

3. Altman, S.P. and Pistiner, J.S., "Velocity Vector Direction Changes for Coplanar Orbital Transfer", Preprint No. 61-75, AAS Fourth Western Regional Meeting, San Francisco, California, August 1961.

4. Pistiner, J.S., "Some Characteristics of the Planar Satellite Orbit", ARS Journal, Vol. 30, No. 3, March 1960, pp. 275-277.

5. Altman, S.P. and Pistiner, J.S., "Hodograph Transformations and Mapping of the Orbital Conics", ARS Journal, Vol. 32, No. 6., June 1962, pp. 1109-1111.

6. Altman, S.P. and Pistiner, J.S., "Polar Hodograph for Ballistic Missile Trajectories", ARS Journal, Vol. 31, No. 11, November 1961, pp. 1592-1594.

7. Altman, S.P. and Pistiner, J.S., "Comment on the Correlation of Stark's Two-Terminal Trajectory Optimization With an Orbital Hodograph Analysis", ARS Journal, Vol. 32, No. 7, July 1962, p. 983.

8. Altman, S.P. and Pistiner, J.S., "Minimum Velocity Increment Solution for Two-Impulse Coplanar Orbital Transfer", AIAA Journal, Vol. 1, No. 2, February 1963, pp. 435-442.

9. Altman, S.P. and Pistiner, J.S., "Analysis of the Orbital Transfer Problem in Three-Dimensional Space", forthcoming AIAA Astrodynamics Conference paper, United Aircraft SCTM 154, March 1963.

10. Altman, S.P., and Pistiner, J.S., "Comment on Invariant Two-Body Velocity Components", AIAA Journal, Vol. 1, No. 5, May 1963, p. 1235.

11. "Proposal for The Acceleration Hodograph and Its Application to Space Trajectory Analysis", United Aircraft SCP 6211, May 4, 1962.

12. Altman, S.P., and Gilbert, A.C., "Variable Transformations for the Analysis of Space Flight Trajectories", XIIIth International Astronautical Congress, Varna, Bulgaria, September 1962.

13. Goldstein, H., "Classical Mechanics", Addison-Wesley Press (1950).

14. Bottaccini, M., "An Alternate Interpretation of Newton's Second Law", AIAA Journal, Vol. 1, No. 4, April 1963, pp. 927-928.

15. Corben, H.C., and Stehle, P., "Classical Mechanics", John Wiley & Sons (1960).

16. MacMillan, W.D., "Statics and Dynamics of a Particle", Dover (1958).

17. Whittaker, E.T., "A Treatise of the Analytical Dynamics of Particles and Rigid Bodies", Cambridge University Press, Dover Printing (1959).

18. Coffin, J.G., "Vector Analysis", John Wiley and Sons (1911).

19. Lockwood, E.H., "A Book of Curves", Cambridge University Press (1961).

20. Encyclopaedia Britannica, Vol. 6; Curves, Special, pp. 887-899.

21. Benney, D.J., "Escape From a Circular Orbit Using Tangential Thrust", Jet Propulsion, Vol. 28, No. 3, March 1958, pp. 167-169.

22. Citron, S.J., Dunin, S.E., and Meissinger, H.F., "A Self-Contained Terminal Guidance Technique for Lunar Landing", ARS 17th Annual Meeting, Preprint No. 2685-62.

23. Andronow, A.A. and Chaikin, C.E., "Theory of Oscillations", Princeton University Press (1949).

24. Smith, G.L. and Schmidt, S.F., "The Application of Statistical Filter Theory to Optimal Trajectory Determination On Board a Circumlunar Vehicle", Preprint No. 61-92, AAS Fourth Western Regional Meeting, San Francisco, California, August 1961.

25. Smith, F.T., "Optimization of Multistage Orbit Transfer Processes by Dynamic Programming", ARS Journal, Vol. 31, No. 11, November 1961, pp. 1553-1559.

26. Wen, L.W., "A Unified Treatment of Variation of Parameters and Differential Expressions Methods in Trajectory Prediction and Error Analysis", Journal of the Aerospace Sciences, Vol. 29, No. 1, Jan. 1962, pp. 61-66, 120.

27. Blitzer, L., Weisfeld, M. and Wheelon, A.D., "Perturbations of a Satellite's Orbit Due to the Earth's Oblateness", Journal of Applied Physics, Vol. 27, No. 10, Oct. 1956, pp. 1141-1149.

28. Blitzer, L. and Wheelon, A.D., "Oblateness Perturbation of Elliptical Satellite Orbits", Journal of Applied Physics, Vol. 28, No. 2, Feb. 1957, p. 279.

29. Blitzer, L., "Apsidal Motion of an IGY Satellite Orbit", Journal of Applied Physics, Vol. 28, No. 11, Nov. 1959, p. 1362.

30. Jacobi, C.G.J., "Vorlesungen über Dynamik" G. Reimer (Berlin), 2nd Edition, 1884, Lecture 16.

31. Crisp, J.D.C., "On The Dynamics of Atmospheric Entry and Reentry", Polytechnic Institute of Brooklyn (PIBAL) Report no. 562, April 1960.

XII. NOMENCLATURE

a	scalar of the total acceleration vector $\bar{a}$
a'	semimajor axis of the instantaneous orbit
Δa	unit-mass acceleration due to applied thrust
C	scalar hodograph parameter of an instantaneous orbit
$\bar{C}$	hodograph vector of an instantaneous orbit ($= \bar{r} \times \bar{v}$) always directed normal to the instantaneous orbital plane
c,d	coefficients for the polar equation of the limaçon
E	system energy of orbital point-mass motion
e	eccentricity of the instantaneous orbit
F	scalar of the total force vector $\bar{F}$
f	scalar of the force vector $\bar{f}$, due to thrust only
i	incidence angle between the orbital plane and the equatorial plane of the celestial body
$\bar{i}, \bar{j}$	orthogonal unit vectors of a rotating polar coordinate system in one plane
J	first coupling constant of the spherical harmonic expansion for the gravitational potential of the celestial body, described as an oblate spheroid
K	constant
k	constant mass-flow rate
L	Lagrangian
l	total angular momentum of the vehicle center-of-mass
m	system mass
n	mean angular velocity of the vehicle in orbit
P	point in space
p	semilatus rectum of the instantaneous orbit

φ	scalar of the radius vector of the limaçon
Q_i	generalized force component
q_i	generalized coordinate
R	scalar hodograph parameter of an instantaneous orbit
$\bar{R}$	hodograph vector of an instantaneous orbit, always directed parallel to the instantaneous apsidal line in the perigeal sense
r	scalar of the radius vector $\bar{r}$ originating at the center of the celestial body
$\mathcal{R}$	radius of curvature
s	scalar of the path vector $\bar{s}$
T	scalar of the thrust vector $\bar{T}$
t	time
U	kinetic energy of orbital point-mass motion
u	slope of the tangent line to the acceleration hodograph at the given point of orbit
V	scalar potential function of the celestial body
v	scalar of the vehicle system velocity vector $\bar{v}$
v_g	exhaust gas velocity
v_n	velocity vector component normal to the radius vector in the instantaneous orbital plane (positive sense toward the orbital flight direction)
v_r	velocity vector component along the radius vector (positive sense outward from the celestial body center)
W	velocity-dependent potential function
X,Y	rectilinear coordinates fixed in inertial space
α	density coefficient
β	angle between the hodograph v_n- axis and the hodograph total velocity

γ angle between the hodograph v_η- axis and the hodograph radius R to the orbital body point on the hodograph

η latitude angle from the equatorial plane of the celestial body

θ angle between the total velocity vector and the local horizon in the orbital plane

θ' angle between the tangent line to a point on the acceleration hodograph, and the normal line to the radius vector at that point

λ parametric variable

μ gravitational constant for the celestial body

N direction of radius vector $\bar{r}$

ν angle between the radius vector (whose direction only is defined by the line N) and an arbitrary reference line fixed in inertial space

ρ scalar of the total acceleration of an orbital vehicle

σ atmospheric density function

τ angle between tangent line to a point on the acceleration hodograph and the abscissa axis

ϕ true anomaly of the vehicle in instantaneous orbit

Ψ apsidal line of the instantaneous orbit at perigee

$\Delta\Psi$ rotation of the apsidal line of an orbit

ψ angle between the radius to a point on the acceleration limacon and the tangent line at that point $\left(=\frac{\pi}{2}-\theta'\right)$

$\Delta\Omega$ rotation of the nodal line of an orbit

Superscripts

$(\sim)$ per unit mass of the ( ) - term

$(-)$ vector quantity

$(\cdot)$ first time derivative of the ( ) - term

$(\cdot\cdot)$ second time derivation of the ( ) - term

Subscripts

b	ballistic
c	circular
d	drag force
e	celestial body surface
f	final
i	initial
J	due to the coupling constant J of the harmonic expansion of the potential field of an oblate spheroid
m	mass
o	reference value
p	powered
r	radial
x,y	rectilinear coordinates fixed in inertial space
ν,n	normal
ϕ	derivative with respect to ϕ

APPENDIX A
PROBLEM STATEMENT FOR LUNAR LANDING TRAJECTORY

The lunar landing trajectory which comprises the specified application problem for this research study is defined by the following thrust program, initial and final conditions, as presented by NASA.

A. Thrust Program

The vector direction of thrust is always in direct opposition (i.e., at 180 degrees) to the velocity vector. The thrust magnitude is constant, and is given together with relevant problem constants, as follows:

1. T = 6000 pounds
2. Specific impulse = 305 seconds
3. Lunar radius = 5,702,000 feet
4. Lunar surface gravity = 5.32 feet per second^2
5. Terrestrial surface gravity = 32.17 feet per second^2

B. Initial Conditions

The vehicle is at the perigee of an elliptical orbit when thrust inception occurs, defined by the following nominal initial data:

1. $\dot{r}$ = 0
2. $r\dot{\nu}$ = 5674 feet per second
3. m = 384.5 slugs
4. Altitude = 50,000 feet
5. t = 0

C. Terminal Conditions

The trajectory is terminated when the velocity becomes zero. At that time, the thrust would be shut down. The nominal terminal conditions obtained with machine solution of the classical equations of motion are as follows:

1. $\dot{r} = 0$

2. $r\dot{\nu} = 0$

3. $m = 211.4$ slugs

4. Altitude = 5467 feet

5. $t = 283$ seconds

For comparative evaluation of the machine solutions with a classical equation program and with a hodograph equation program, the following equations and endpoint conditions were used by the UA staff for programming and machine solution:

1. Classical Equations

$$m = m_i + \dot{m}t$$

$$2\dot{r}\dot{\nu} + r\ddot{\nu} = \frac{F_\nu}{m}$$

$$\ddot{r} - r\dot{\nu}^2 + \frac{\mu}{r^2} = \frac{F_r}{m}$$

where

$$F_\nu = -T\left(\frac{r\dot{\nu}}{v}\right)$$

$$F_r = -T\left(\frac{\dot{r}}{v}\right)$$

$$v = \sqrt{(\dot{r})^2 + (r\dot{\nu})^2}$$

Initial Conditions:

$\dot{r}$ = 0

$r\dot{\nu}$ = 5673.63 feet per second

r = 5.752×10^6 feet

m_i = 384.507 slugs

$\dot{m}$ = -0.6115055 slugs per second

μ = 172.968×10^{12} feet^3 per second^2

T = 6000 pounds

Terminal Conditions:

$\dot{r} = 0$

$r\dot{\nu} = 0$

2. Hodograph Equations

$$m = m_i + \dot{m}t$$

$$\dot{R}\sin\phi + 2\dot{C}\sin\phi\cos\phi = \frac{F_r}{m}$$

$$\dot{C} + \dot{R}\cos\phi - 2\dot{C}\sin^2\phi = \frac{F_\nu}{m}$$

where

$$F_\nu = -T\left|\frac{C + R\cos\phi}{v}\right|$$

$$F_r = -T\left|\frac{R\sin\phi}{v}\right|$$

$$v = \sqrt{C^2 + R^2 + 2CR\cos\phi}$$

Initial Conditions:

$\phi = 0$

$C = 5300.75697$ feet per second

$R = 373.24303$ feet per second

$m_i = 384.507$ slugs

$\dot{m} = -0.6115055$ slugs per second

$T = 6000$ pounds

Terminal Conditions:

$R\sin\phi = 0$

$C + R\cos\phi = 0$

APPENDIX B
THE ACCELERATION LIMAÇON

The limaçon, a special plane curve ascribed principally to Pascal (Ref. 19 and 20), can be defined by the following polar equation:

$$\rho = c + d\cos\phi \tag{A-1}$$

or by the following parametric equations:

$$x = c\cos\lambda + \frac{d}{2}\cos 2\lambda \tag{A-2}$$

$$y = c\sin\lambda + \frac{d}{2}\sin 2\lambda \tag{A-3}$$

Given a circle of radius = $\frac{d}{2}$, the limaçon may be generated by the geometric construction in Figure B-1. Select a point on the Circle (OAD) as the origin O of a rectilinear coordinate system (X-Y), with one axis along a diameter ($\overline{OD}$). Pass a line through the origin at the required angle ϕ. From the resulting line intersection A with the circle, obtain points B and C, each at a distance = c. The points B and C comprise two points of the limaçon, the complete figure of which is generated for all possible values of ϕ with specified c and d.

The geometric form of the limaçon figure varies with the relative values of the constants c and d, as shown in Figure B-2. The limaçon has many interesting properties, some directly useful in optics. Although these properties of the limaçon will not be presented here, it is noted[1] that the complex variable transformation $w = z^2$ makes circles $|z-b| = c$, (b,c real), in the z-plane correspond to limaçons in the w-plane.

Some characteristic properties of the acceleration limaçon (Equation 64) have been derived and presented in Table B-I, together with basic definitions. These properties are defined as shown in Figure B-3.

---

[1] Phillips, E.G., "Functions of a Complex Variable", Interscience Publishers (1946), pp. 61-62.

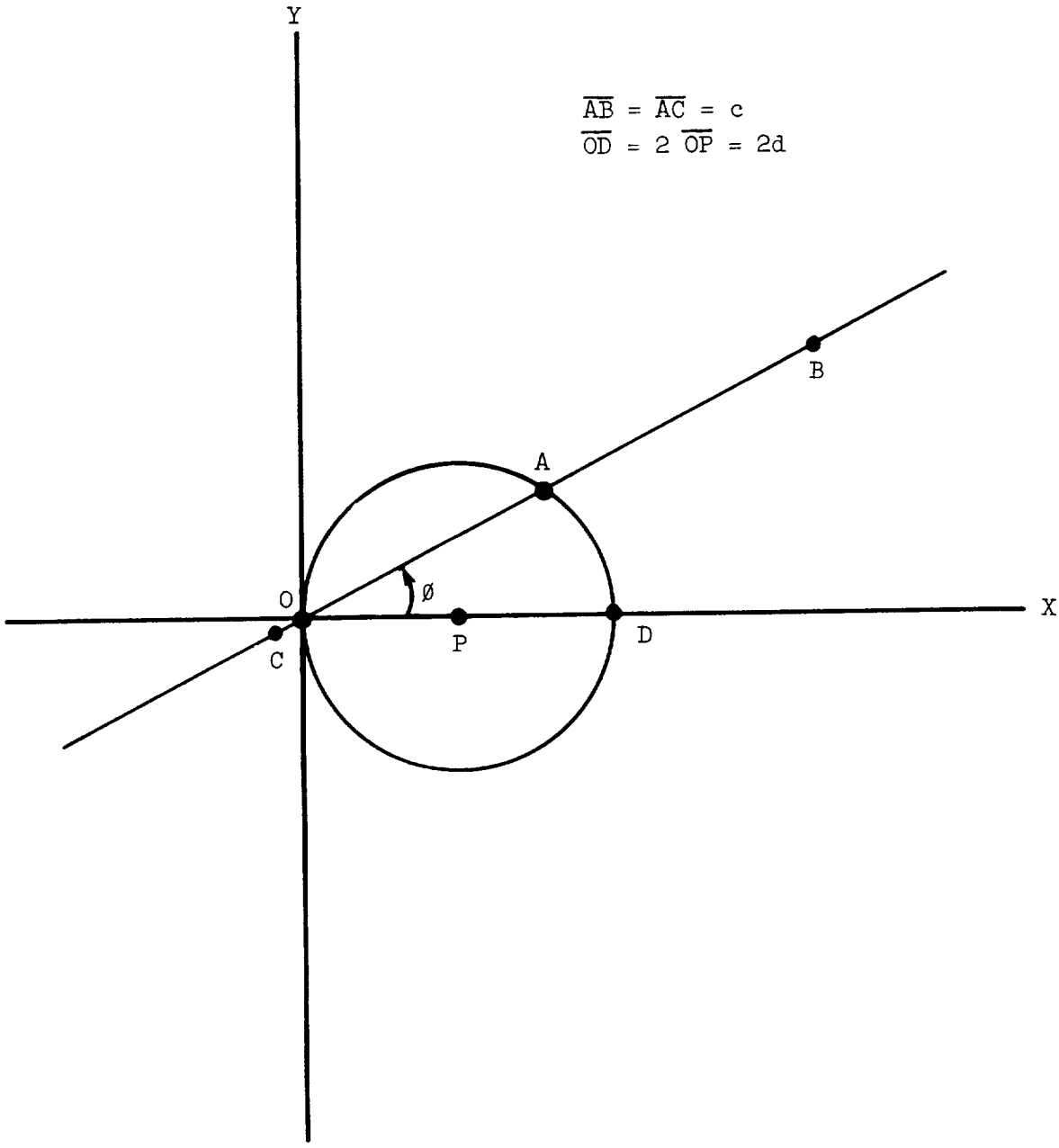

Fig. B-1 Generation of the Limaçon

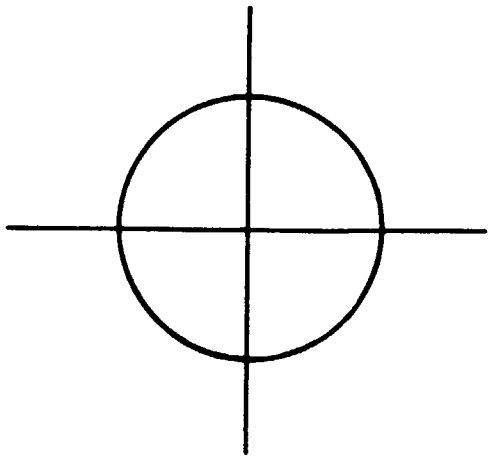

A. d=0

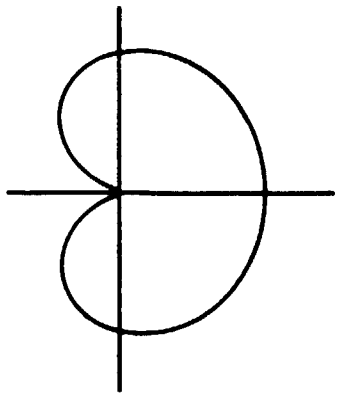

C. c=2d (i.e., cardioid)

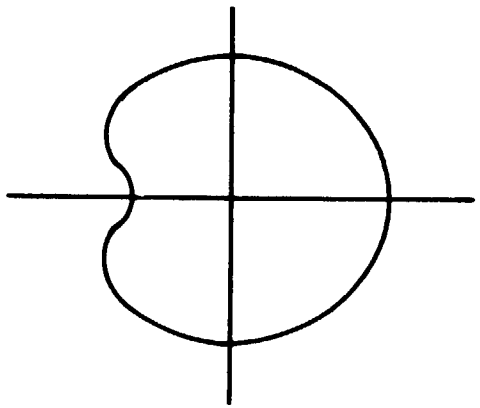

B. c>2d

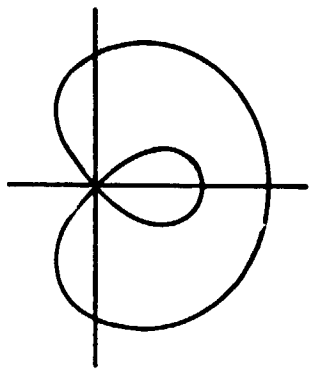

D. c< 2d

Fig. B-2 Various Forms of the Limaçon

TABLE B-I
EQUATIONS FOR THE ACCELERATION LIMAÇON

BASIC DEFINITIONS

$$\rho = (c + d\cos\phi)^2 \tag{A-4}$$

where $c = \frac{C^2}{\sqrt{\mu}}$

$$d = \frac{CR}{\sqrt{\mu}}$$

$$\frac{d}{c} = \frac{R}{C} = e$$

CHARACTERISTIC PROPERTIES

$$\tan\psi = -\frac{c + d\cos\phi}{2d\sin\phi} = -\frac{1 + e\cos\phi}{2e\sin\phi} \tag{A-5}$$

$$\tan\tau = \frac{3d\sin^2\phi - (d + c\cos\phi)}{\sin\phi\,(c + 3d\cos\phi)} = \frac{3e\sin^2\phi - (e + \cos\phi)}{\sin\phi\,(1 + 3e\cos\phi)} \tag{A-6}$$

$$\frac{ds}{d\phi} = \left[\rho\left(\rho + 4d^2\sin^2\phi\right)\right]^{\frac{1}{2}} \tag{A-7}$$

$$\mathcal{R} = \rho^{\frac{1}{2}}\,\frac{\left[(4d^2 + c^2) + 2cd\cos\phi - 3d^2\cos^2\phi\right]^{\frac{3}{2}}}{(6d^2 + c^2) + 4cd\cos\phi - 3d^2\cos^2\phi} \tag{A-8}$$

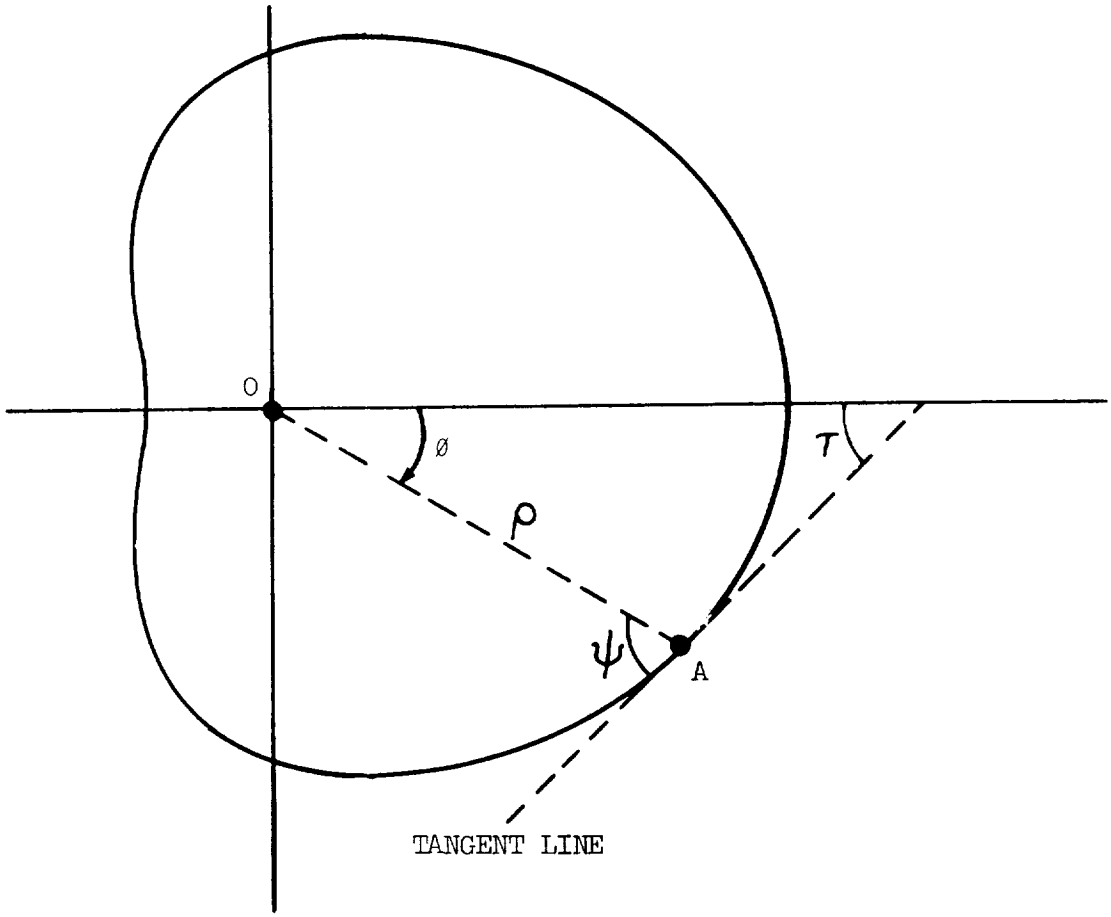

Fig. B-3 Characteristic Properties of the Acceleration Limaçon